cmgh
CELLULAR AND MOLECULAR GASTROENTEROLOGY AND HEPATOLOGY

ORIGINAL RESEARCH

# Up-regulation of Aquaporin 5 Defines Spasmolytic Polypeptide-Expressing Metaplasia and Progression to Incomplete Intestinal Metaplasia

Su-Hyung Lee,[1,2,a] Bogun Jang,[3,a] Jimin Min,[1,2,a] Ela W. Contreras-Panta,[2,7] Kimberly S. Presentation,[1,2] Alberto G. Delgado,[4,5] M. Blanca Piazuelo,[4,5,6] Eunyoung Choi,[1,2,7] and James R. Goldenring[1,2,7,8]

*[1]Section of Surgical Sciences, [2]Epithelial Biology Center, Vanderbilt University Medical Center, Nashville, Tennessee; [3]Department of Pathology, Jeju National University School of Medicine and Jeju National University Hospital, Jeju, Republic of Korea; [4]Division of Gastroenterology, Hepatology, Nutrition, [5]Department of Medicine, [6]Center for Mucosal Inflammation and Cancer, Vanderbilt University Medical Center, Nashville, Tennessee; [7]Department of Cell and Developmental Biology, Vanderbilt University School of Medicine, Nashville, Tennessee; and [8]Nashville VA Medical Center, Nashville, Tennessee*

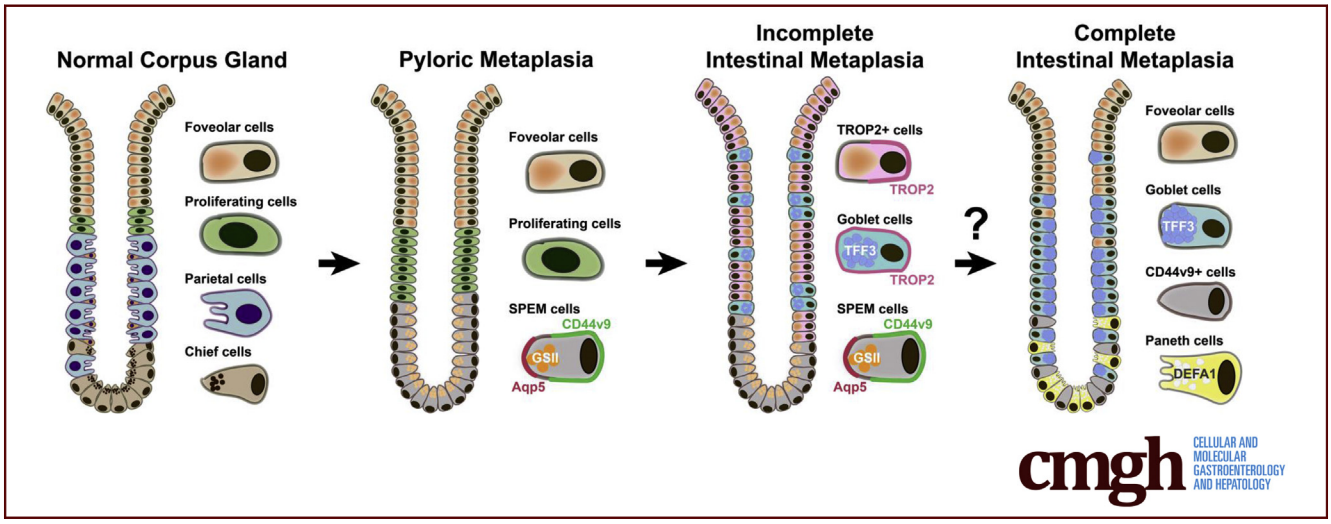


## SUMMARY

We have identified aquaporin 5 (AQP5) as a specific marker of SPEM in both mouse and human gastric corpus. In human stomach, AQP5-expressing SPEM cells are present at the bases of glands with incomplete, but not complete, intestinal metaplasia.

**BACKGROUND & AIMS:** Metaplasia in the stomach is highly associated with development of intestinal-type gastric cancer. Two types of metaplasias, spasmolytic polypeptide-expressing metaplasia (SPEM) and intestinal metaplasia (IM), are considered precancerous lesions. However, it remains unclear how SPEM and IM are related. Here we investigated a new lineage-specific marker for SPEM cells, aquaporin 5 (AQP5), to assist in the identification of these 2 metaplasias.

**METHODS:** Drug- or *Helicobacter felis* (*H felis*) infection-induced mouse models were used to identify the expression pattern of AQP5 in acute or chronic SPEM. Gene-manipulated mice treated with or without drug were used to investigate how AQP5 expression is regulated in metaplastic lesions. Metaplastic samples from transgenic mice and human gastric cancer patients were evaluated for AQP5 expression. Immunostaining with lineage-specific markers was used to differentiate metaplastic gland characteristics.

**RESULTS:** Our results revealed that AQP5 is a novel lineage-specific marker for SPEM cells that are localized at the base of metaplastic glands initially and expand to dominate glands after chronic *H felis* infection. In addition, AQP5 expression was up-regulated early in chief cell reprogramming and was promoted by interleukin 13. In humans, metaplastic corpus showed highly branched structures with AQP5-positive SPEM. Human SPEM cells strongly expressing AQP5 were present at the bases of incomplete IM glands marked by TROP2 but were absent from complete IM glands.

**CONCLUSIONS:** AQP5-expressing SPEM cells are present in pyloric metaplasia and TROP2-positive incomplete IM and may be an important component of metaplasia that can predict a higher risk for gastric cancer development. *(Cell Mol*

*Gastroenterol Hepatol 2022;13:199–217; https://doi.org/10.1016/j.jcmgh.2021.08.017)*

*Keywords:* AQP5; Gastric Cancer; IM; TROP2; SPEM.

Metaplasia is recognized as a precursor lesion of many types of gastrointestinal tract cancers.[1–4] In gastric cancer, metaplasia first appears in the setting of acute and chronic gastritis as a response to physical or chemical damage to the mucosa. Two types of metaplasias, pyloric metaplasia and intestinal metaplasia (IM), are observed in the human stomach.[5–7] Pyloric metaplasia is initiated from spasmolytic polypeptide-expressing metaplasia (SPEM) cells, which first arise from transdifferentiation of zymogen granule-secreting chief cells in response to acute mucosal damage and oxyntic atrophy.[8,9] As a component of pyloric metaplasia, SPEM cells represent a reversible and reparative metaplasia. Therefore, pyloric metaplasia with SPEM cells can give way to the return of normal oxyntic glands during repair of the damaged mucosa.[7] With chronic inflammation or injury, SPEM can also progress to IM, which can represent a more severe type of metaplasia.[10,11] This SPEM to IM conversion indicates that the metaplasia has passed an inflection point for preneoplastic metaplasias that may progress to dysplasia and adenocarcinoma.

Although the gastric cancer risk is increased in human patients with metaplasias, the presence of metaplasias is not always an absolute factor for gastric cancer development. H&E staining and other histochemical/immunohistochemical methods have been used for identification and classification of metaplasias and for the identification of markers associated with higher gastric cancer risk.[12] Metaplasia arises as a focal process initiated in single glands, and isolated metaplastic glands can be identified in an otherwise normal corpus mucosa.[13] However, in a field of metaplasia, different types of metaplastic glands can be arranged in neighboring focal lesions forming a complex aggregate of glands with mixtures of gastric or intestinal cell lineages, which are co-positive for multiple cell lineage markers. Although a number of cell lineage markers including human epididymis protein 4 (HE4), trefoil factor (TFF)2, MUC6, or CD44v9 for SPEM and TFF3, MUC2, caudal type homeobox (CDX)1/2, or alpha defensing 5 (DEFA5) for IM have been considered to determine the identities of metaplasias, it is not clear how the various glandular components are distributed in different types of metaplastic glands and whether any lineage-specific markers or marker combinations can more definitively distinguish the metaplastic gland types that may be associated with a higher risk of gastric cancer development.

Aquaporin (AQP) proteins are a large family of water transporters, present in the cell membranes, which may be involved in cancer progression.[14–16] Several AQPs have previously been identified in stomach tissues. AQP4 is present in acid-secreting parietal cells localized in the distal corpus area and may be associated with gastric carcinogenesis.[17,18] AQP3 is not present in normal stomach mucosa, but it is observed in the membranes of goblet cells present in IM as well as in gastric cancer tissues and may have roles in cancer progression and metastasis.[19,20] AQP5 is specifically present in deep antral gland mucous cells and antral stem/progenitor cells in the distal stomach[21,22] and is up-regulated in gastrointestinal tract cancers.[16] In our previous study, we found that the AQP5 transcripts were enriched 4.6-fold in SPEM but decreased to 1.3-fold in IM compared with normal chief cells.[23] These data suggested that AQP5 is up-regulated in specific metaplastic lineages in the corpus of the stomach. In this study, we have therefore investigated the relationship of AQP5 expression with the metaplasia development and progression in various mouse models and human patient stomach tissues using a co-immunostaining method for multiple markers. We have also evaluated the distribution of AQP5 protein expression in different types of cell lineages in metaplastic glands as an important metaplastic gland component during metaplasia progression.

## Results

### *AQP5 Expression Is Induced in Gastric Intrinsic Factor–Positive Cells During Epithelial Injury or Recovery in Mice*

Recently, Tan et al[22] suggested that AQP5 represents a marker for resident stem cells in the gastric antrum and also is expressed in deep antral gland mucous cells, whereas no expression of AQP5 was observed in the normal corpus. We similarly observed no significant expression of AQP5 in the normal mouse corpus (Figure 1*A* and *C*). L635 treatment induces rapid parietal cell death and induces the emergence of SPEM through chief cell transdifferentiation.[8] AQP5 expression emerged in gastric intrinsic factor (GIF)-positive chief cells at the bases of gastric corpus glands showing that 6.6% of GIF-positive glands contained AQP5-expressing cells after L635 treatment for 1 day to induce acute parietal cell loss. AQP5 positivity of GIF-expressing cells in corpus glands significantly increased after extended epithelial damage by multiple doses of L635 (13.0% at day 2 and 33.8% at day 3; Figure 1*A* and *C*). The proportion of the gland containing GIF-expressing chief cells was decreased after multiple doses of L635 treatment as described previously, but we observed GIF-positive cells with proliferative activity (Ki67 positivity), which was considerably enhanced

[a]Authors share co-first authorship.

***Abbreviations used in this paper:*** **AQP, aquaporin; CDX, caudal type homeobox; DAPI, diamidino-2-phenylindol; DEFA5, alpha defensin 5; GIF, gastric intrinsic factor; GSII, *Griffonia simplicifolia* II; HE4, human epididymis protein 4; *H felis*, *Helicobacter felis*; HID/AB, high-iron diamine/Alcian blue; IL, interleukin; ILC2, type 2 innate lymphoid cell; IM, intestinal metaplasia; PAS, periodic acid-Schiff; SPEM, spasmolytic polypeptide-expressing metaplasia; TFF, trefoil factor; TROP2, trophoplast antigen 2; xCT, cystine/glutamate antiporter.**

Most current article



2352-345X
https://doi.org/10.1016/j.jcmgh.2021.08.017

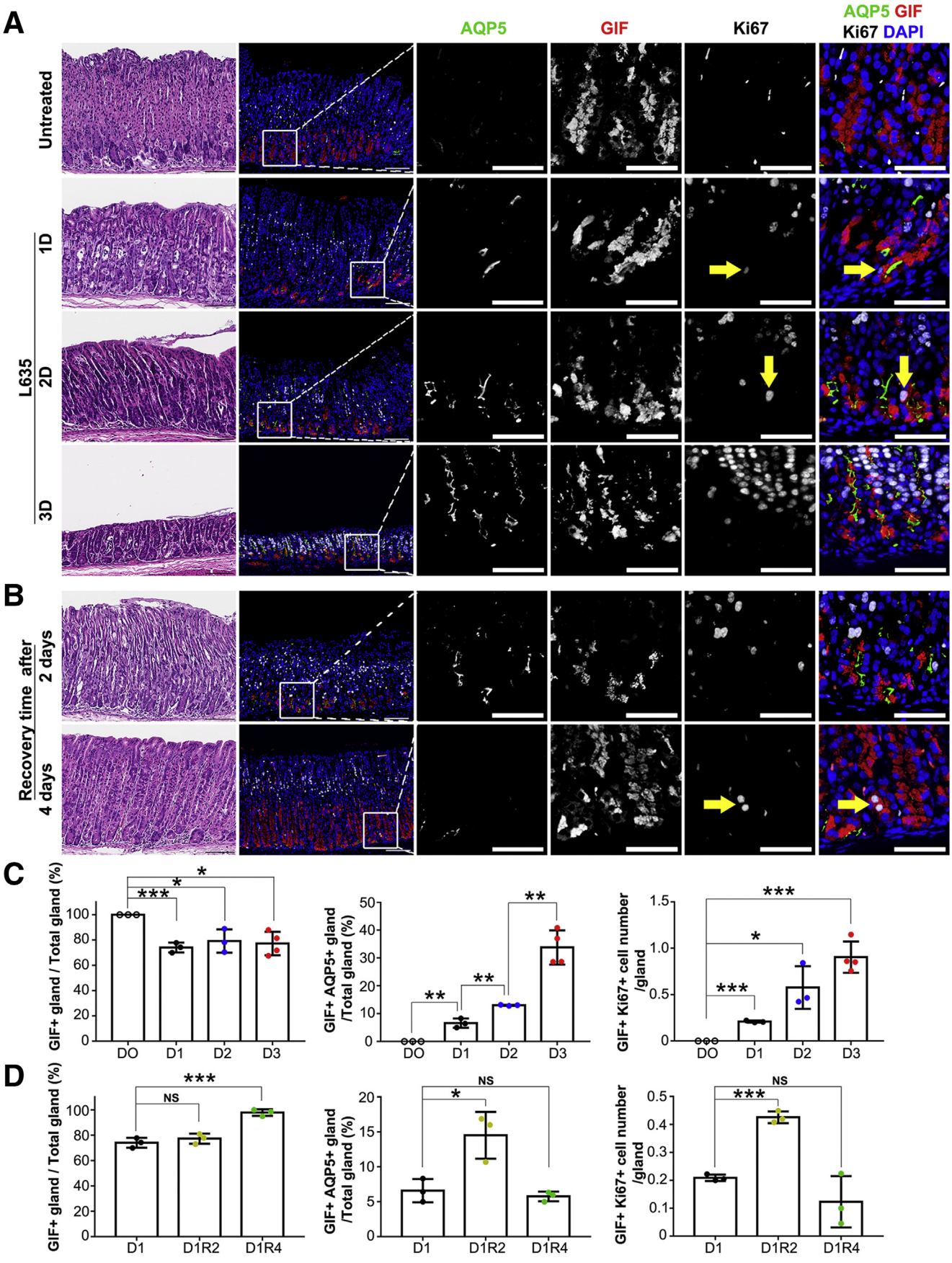
A
AQP5
GIF
Ki67
AQP5 GIF
Ki67 DAPI
Untreated
L635
1D
2D
3D
B
Recovery time after
2 days
4 days
C
GIF+ gland / Total gland (%)
GIF+ AQP5+ gland /Total gland (%)
GIF+ Ki67+ cell number /gland
DO
D1
D2
D3
D
D1
D1R2
D1R4
NS

by additional L635 treatments (Figure 1*A* and *C*). These data indicate that parietal cell loss can induce not only AQP5 expression but also proliferative activity of GIF-positive chief cells as an early response to epithelial damage.

We also examined AQP5 expression in GIF-expressing chief cells during recovery after damage. Compared with L635-treated stomach for 1 day, AQP5-expressing chief cells in the corpus were increased over 2-fold after recovery for 2 days (Figure 1*A*, *B*, and *D*). However, 4 days after recovery, the number of AQP5- and GIF-co-positive cells returned to the same level as in stomachs of mice treated with L635 for 1 day (Figure 1*A*, *B*, and *D*). The proliferative activity of chief cells was also enhanced after recovery for 2 days (Figure 1*A*, *B*, and *D*) and then decreased over time, but a few GIF-positive chief cells still showed nuclear Ki67 positivity at 4 days after recovery (1*A*, *B*, and *D*). Therefore, AQP5 expression in chief cells remains up-regulated early in the recovery period.

## AQP5 Is Expressed in Mouse Models of SPEM Induction

On the basis of the result that AQP5 expression gradually increased in chief cells during SPEM development after L635-induced parietal cell loss, we therefore examined AQP5 expression with other markers described previously in SPEM in the gastric corpus. We have previously shown that the parietal cell protonophore drug L635 induces oxyntic atrophy and SPEM within 3 days of oral administration[8] with prominent expression of CD44v9.[24] In the L635 treatment model, one dose of L635 treatment elicited basolateral expression of CD44v9 in chief cells at the bases of corpus glands, and some of the cells also demonstrated apical AQP5 positivity and *Griffonia simplicifolia* II (GSII) positivity, indicative of early formation of SPEM (Figure 2*A*). CD44v9-positive SPEM cells were widely present at the bases of gastric corpus glands after 2 dosages of L635-treated stomach, and these cells were also positive for AQP5 as well as GSII. Corpus glands after 3 dosages of L635 showed significantly increased AQP5 expression along with CD44v9 positivity compared with that in other groups (Figure 2). Furthermore, the proportion of the AQP5-positive gland was increased over 3-fold, and AQP5- and GSII-co-positive glands were increased about 5-fold compared with the gastric mucosa after 2 doses of L635 (Figure 2*B*).

We have also described a second model of acute oxyntic atrophy with the drug DMP-777, which induces SPEM over a longer time course and is associated with little detectable immune cell infiltrate.[25,26] In accordance with the L635-induced SPEM model, DMP-777 treatment caused acute parietal cell loss, resulting in SPEM development, although over a longer time course. DMP-777–treated stomachs showed CD44v9-expressing SPEM cells, which were also positive for GSII and AQP5 beginning at 7 days of treatment and most prominently after 14 days of treatment (Figure 3*A* and *C*). AQP5 expression increased incrementally over time during DMP-777 treatment (Figure 3*B*), indicating that AQP5 can specifically define the development of the SPEM cell lineage.

In addition to the drug-induced acute SPEM models, we examined AQP5 expression in acetic acid-induced gastric injury and chronic SPEM caused by *Helicobacter felis* (*H felis)* infection. In contrast to unaffected gastric glands showing no expressions of GSII, CD44v9, or AQP5 at the base, regenerating glands adjacent to ulcerated mucosa prominently showed CD44v9 expression at the base as described previously (Figure 4*A*).[27] Most of the CD44v9-expressing basal gland cells strongly expressed AQP5 and GSII (Figure 4*A*). These findings indicate that AQP5 is expressed in SPEM lineages as part of the regenerative mucosa surrounding acute ulcers. In chronic *H felis* infection model most of the glands in the *H felis*-infected corpus demonstrated GSII-positive SPEM cells with minimal or no foveolar hyperplasia at 12 months after infection. The SPEM cells in almost the entire gland were also strongly stained with apical AQP5 as well as basolateral CD44v9 (Figure 4*B*). These data suggest that AQP5 is continuously expressed in SPEM cells during chronic inflammation.

## Analysis of AQP5 Expression During Reprogramming of Chief Cells Into SPEM Cells

We previously demonstrated in mouse models that transdifferentiation of chief cells into SPEM proceeds with an orderly set of transitions that are initiated by a cascade of interleukin (IL) 33 and IL13 release[28,29] and the up-regulation of CD44v9 and the cystine/glutamate antiporter (xCT) cystine transporter to protect cells from reactive oxygen species.[24] Therefore, we sought to identify how AQP5 expression is altered in mice with manipulation of these key regulators. In mice with deletion of ST2, the receptor for IL33, after L635 treatment only weak expression of CD44v9 expression was observed in chief cells at the bases of corpus glands, in accordance with previous results,[28] and AQP5 expression was rarely observed in the glands (Figure 5*A*). However, both CD44v9 and AQP5 expression reemerged at the base of glands in ST2-deficient mice after treatment with L635 in combination with recombinant IL13 (Figure 5*A*), suggesting IL13 induces AQP5 expression in trans-differentiating chief cells.

We have previously demonstrated that knockout of xCT blocked the completion of chief cell transdifferentiation into

**Figure 1.** (***See previous page***). **AQP5 is expressed in GIF-positive chief cell after L635-induced parietal cell loss and during recovery.** (*A*) H&E and immunofluorescence staining for AQP5, chief cell marker GIF, proliferation marker Ki67, and nuclei marker DAPI in gastric corpus tissues from mice with or without L635 treatment for 1, 2 or 3 days (D1, 2, or 3). *Arrows* indicate Ki67- and GIF-co-positive cells. Scale bar = 100 $\mu$m or 50 $\mu$m (expanded images). (*B*) Immunofluorescence staining for AQP5, GIF, Ki67, and DAPI in gastric corpus tissues from mice with recovery for 2 (D1R2) or 4 (D1R4) days after L635 treatment for 1 day. *Arrow* indicates Ki67- and GIF-co-positive cells. Scale bar = 100 $\mu$m or 50 $\mu$m (expanded images). (*C* and *D*) Quantification of GIF-positive gland, GIF- and AQP5-co-positive gland, or GIF- and Ki67-co-positive cell per ×20 field (n = 3–4) in consecutive L635 treatments (*C*) or during recovery after L635 treatment for 1 day (*D*). **P* < .05, ***P* < .01, ****P* < .001.

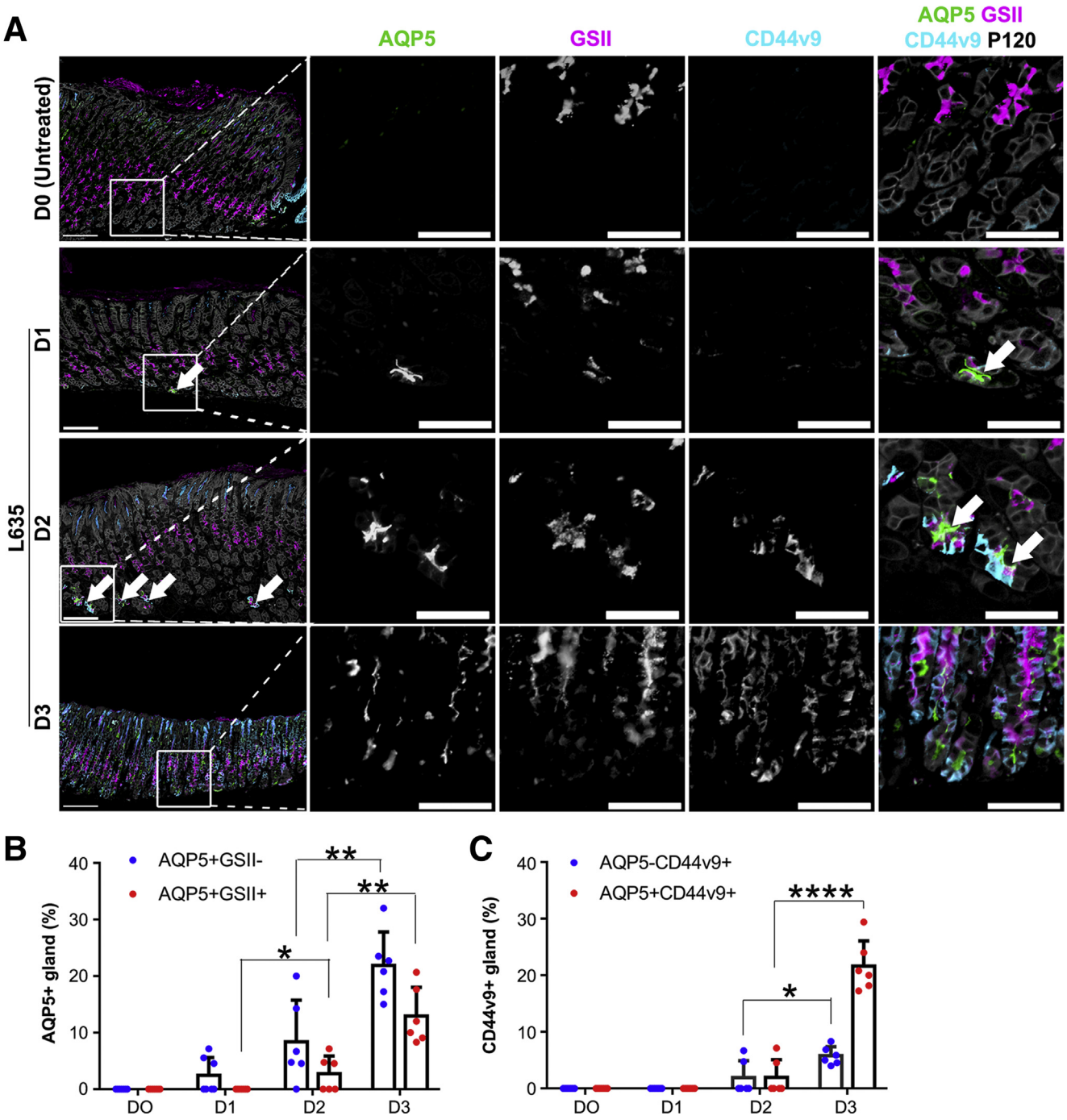


**Figure 2. AQP5 is expressed in L635- and *H felis* infection-induced SPEM in the gastric corpus of mice.** (*A*) Immunofluorescence staining for AQP5, mucus marker GSII-lectin, SPEM marker CD44 variant 9 (CD44v9), and epithelial membrane marker p120 in gastric corpus tissues from mice with or without L635 treatment for 1, 2 or 3 days. *Arrows* indicate AQP5-expressing cells. Scale bar = 100 $\mu$m or 50 $\mu$m (expanded images). (*B*) Quantification of AQP5 single or AQP5 and GSII-lectin co-positive gland per ×20 field (n = 6). AQP5 expression was first observed at the base of a few glands of mice treated with L635 for 1 day without GSII expression. Over time, the numbers of AQP5 single positive or AQP5 and GSII co-positive glands were significantly increased in cells at the bases of glands. *$P < .05$, **$P < .01$. (*C*) Quantification of CD44v9 single or AQP5 and CD44v9 co-positive gland per ×20 field (n = 6). CD44v9-expressing glands were prominently observed after L635 treatment for 3 days. Most of these glands co-expressed AQP5. *$P < .05$, ****$P < .0001$.

SPEM.[24] Importantly, xCT deletion did not significantly inhibit up-regulation of AQP5 in transdifferentiating chief cells (Figure 5*B*), although xCT knockout mice did show less prominent CD44v9 expression after L635 treatment compared with the pattern in treated wild-type mice. Thus, up-regulation of AQP5 expression is an early alteration in transdifferentiating

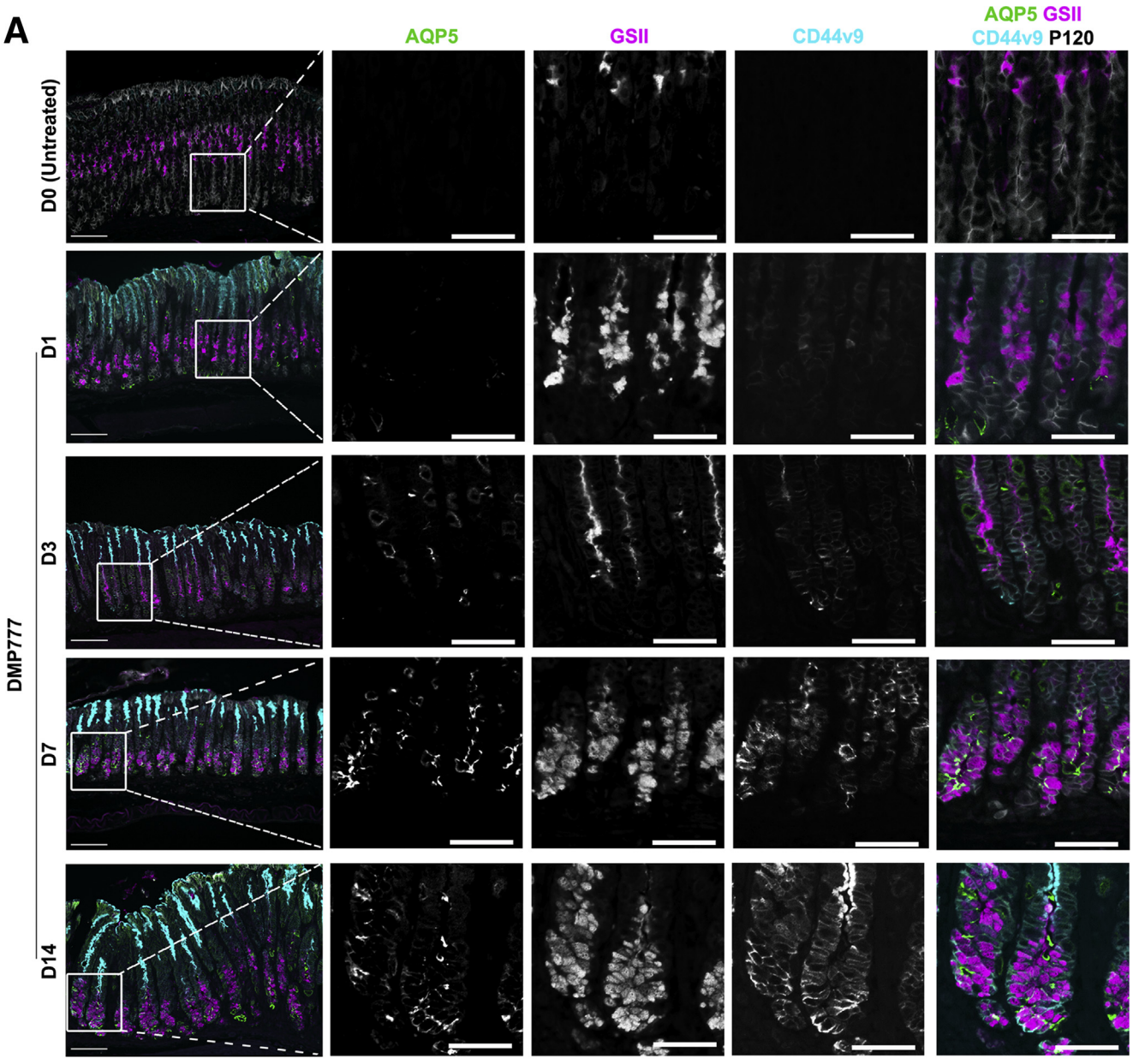
A
AQP5
GSII
CD44v9
AQP5 GSII
CD44v9 P120
D0 (Untreated)
D1
D3
D7
D14
DMP777

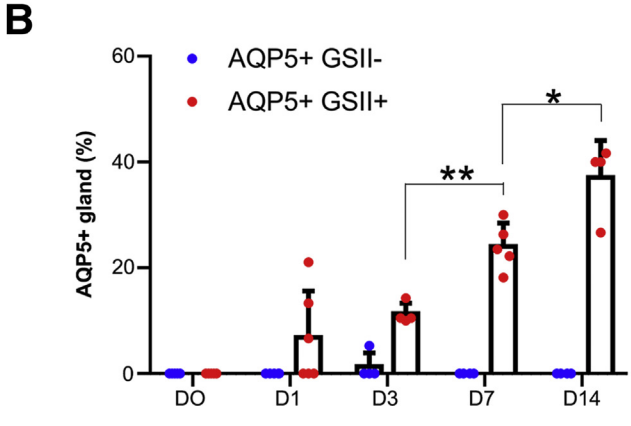
B
AQP5+ GSII-
AQP5+ GSII+
AQP5+ gland (%)
60
40
20
0
DO
D1
D3
D7
D14
**
*

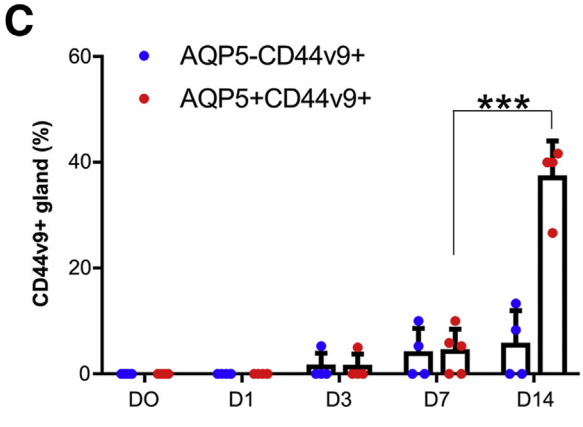
C
AQP5-CD44v9+
AQP5+CD44v9+
CD44v9+ gland (%)
60
40
20
0
DO
D1
D3
D7
D14
***

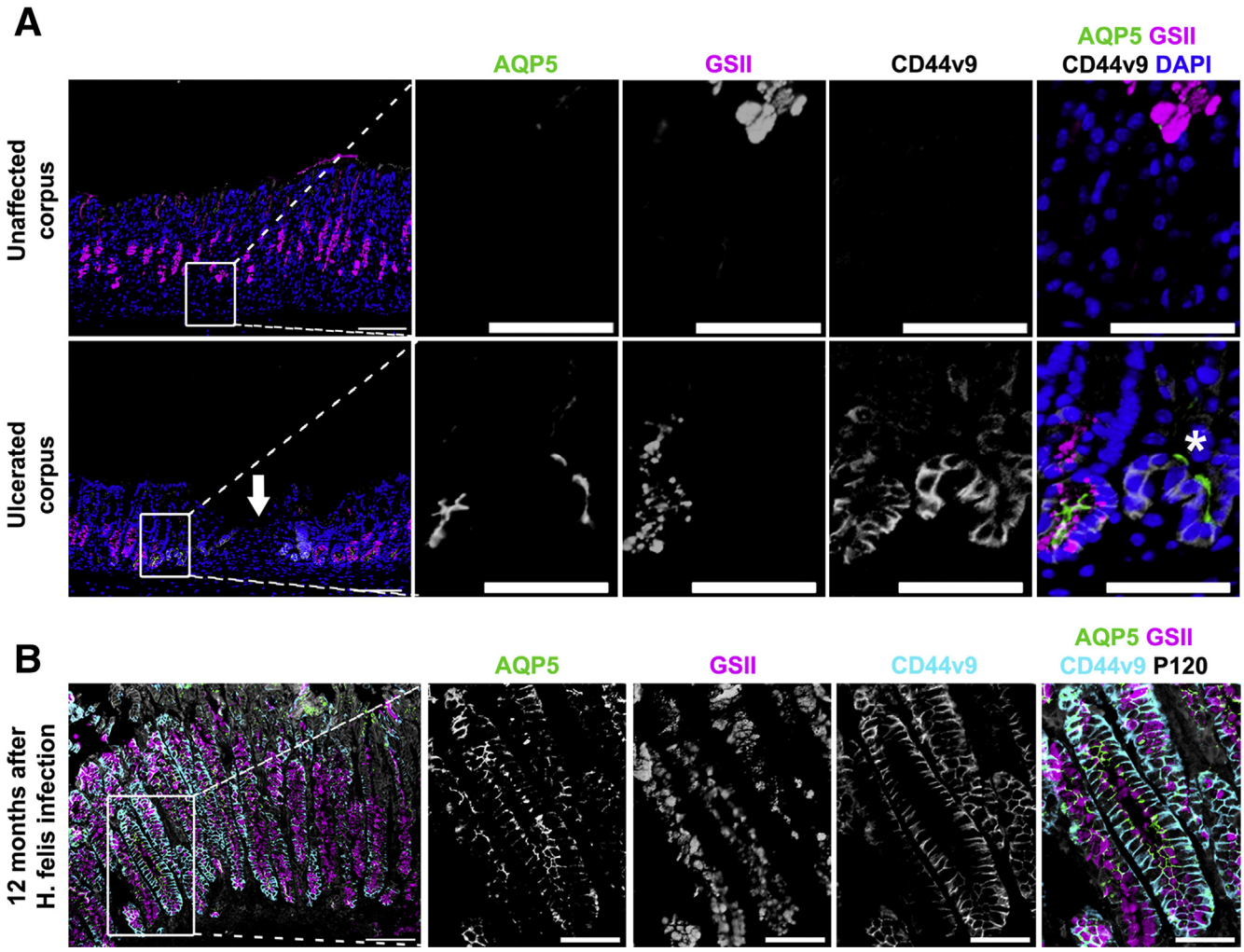


**Figure 4. AQP5 is up-regulated in SPEM associated with acute acetic acid ulcers and chronic *H felis* infection.** *(A)* Immunofluorescence staining for AQP5, mucus marker GSII-lectin, SPEM marker CD44v9, and nuclei marker DAPI in gastric corpus tissues from acetic acid-induced injury. *Arrow* indicates ulcerated gastric mucosa. Note in the expanded images 2 glands showing different expression patterns for GSII-lectin. Gland nearest to the ulcerated region, indicated by *asterisk*, did not show GSII-lectin, but both showed AQP5 expression. Scale bar = 100 $\mu$m or 50 $\mu$m (expanded images). (*B*) Immunofluorescence staining for AQP5, GSII-lectin, CD44v9, and epithelial membrane marker p120 in gastric corpus tissues from *H felis*-infected mice. Apical AQP5 expression is seen throughout SPEM cells. Scale bar = 100 $\mu$m or 50 $\mu$m (expanded images).

chief cells induced by a signaling cascade of IL33 and IL13, which is ultimately sustained in SPEM (Figure 5*C*).

## AQP5 Is Expressed in Metaplasia Induced by Kras Activation in Mice

Previously, we reported a mouse model showing the full spectrum of metaplasia from SPEM to IM to dysplasia in mice with induced expression of Kras in Mist1-positive chief cells (Mist1-Kras mice).[30] Mist1-Kras mice demonstrate SPEM lineages at 1 month after induction, with TFF3-expressing IM developing after 3 months and progression to dysplasia by 4 months after induction.[30] In the present study, we examined the co-expression of AQP5 with other lineage markers over a time course after active Kras induction. One month after active Kras induction, corpus glands at the base prominently showed co-expression of AQP5 and GSII expression in SPEM cells (Figure 6). After 3

**Figure 3. (*See previous page*). AQP5 is expressed in DMP777-induced SPEM in gastric corpus of mice.** (*A*) Immunofluorescence staining for AQP5, mucus marker GSII-lectin, SPEM marker CD44v9, and epithelial membrane marker p120 in gastric corpus tissues from mice without or with DMP777 treatment for 1, 3, 7 or 14 days. Scale bar = 100 $\mu$m or 50 $\mu$m (expanded images). (*B*) Quantification of AQP5 single or AQP5 and GSII-lectin co-positive gland per ×20 field (n = 4–6). AQP5 expression was first observed at the base of a few glands in mice treated with DMP-777 for 3 days with small amount of GSII co-expression. Over time, the numbers of AQP5 and GSII-lectin co-positive glands were significantly increased at the bases of glands. $^{*}P < .05$, $^{**}P < .01$. (*C*) Quantification of CD44v9 single or AQP5 and CD44v9 co-positive glands per ×20 field (n = 4–6). CD44v9 expression was observed at the base of few glands after DMP-777 treatment for 7 days, but it was markedly increased at 14 days of treatment with AQP5 co-expression. $^{***}P < .001$.

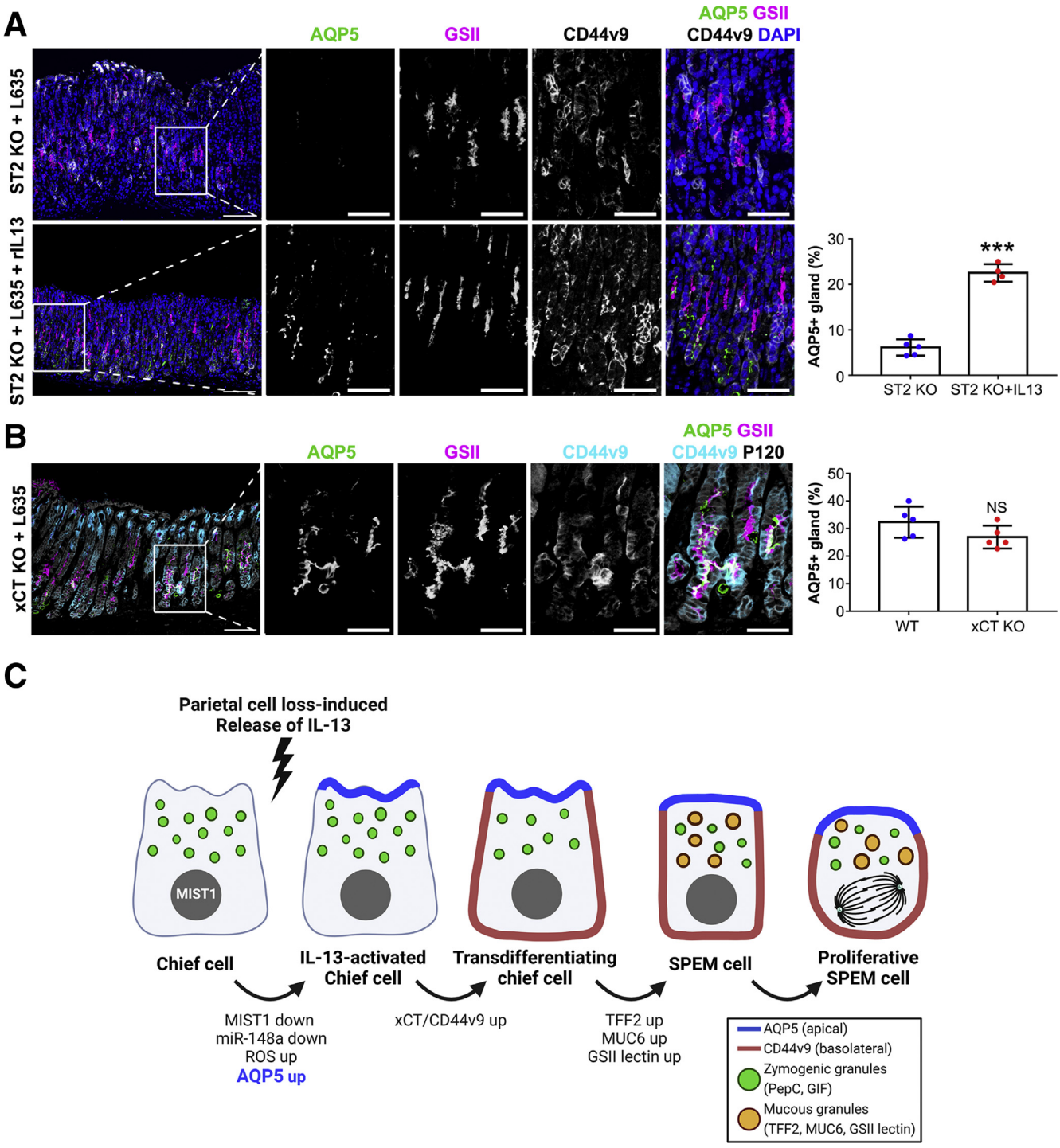


**Figure 5. AQP5 expression is up-regulated by signaling cascade of IL33 receptor, ST2, and IL13, but not affected by xCT knockout (KO).** (*A*) Immunofluorescence staining for AQP5, mucus marker GSII-lectin, SPEM marker CD44v9, and nuclei marker DAPI in gastric corpus tissues from L635-treated ST2 KO mice for 3 days with or without recombinant IL13 injection and quantification of glands with AQP5 expression at the base (n = 4–5). ***$P < .001$. Scale bar = 100 $\mu$m or 50 $\mu$m (expanded images). (*B*) Immunofluorescence staining for AQP5, GSII-lectin, CD44v9, and epithelial membrane marker p120 in gastric corpus tissues from xCT KO mice treated with L635 for 3 days and quantification of gland with AQP5 expression at the base (n = 4–5). Scale bar = 100 $\mu$m or 50 $\mu$m (expanded images). (*C*) Schematic diagram of AQP5 expression in discrete stages of transdifferentiation of chief cells into SPEM. Release of IL13 induced by parietal cell loss is required for AQP5 expression at early stages of transdifferentiation, and AQP5 expression is continuously maintained during whole process of SPEM development. Illustration was created with BioRender.com.

months, the AQP5 and GSII were still present in SPEM cells at the bases of glands, and only a smaller number of GSII and AQP5 co-positive cells remained at the base of glands at 4 months after induction (Figure 6). We have recently reported that the marker trophoplast antigen 2 (TROP2) is upregulated at 3–4 months after the active Kras induction and represents a marker for transition to incomplete IM and dysplasia in the stomach.[31] As previously reported, TROP2 was not present at 1 month after induction but was present in scattered glands at 3 months after induction, and more prominent expression was observed in metaplastic and dysplastic glands at 4 months after induction (Figure 6). Importantly, AQP5 was not present in cells expressing TROP2. These findings suggest the association of SPEM lineages at the bases of glands with an incomplete IM phenotype.

## AQP5 Is Expressed in Human SPEM and in the Normal Antrum, but not in the Normal Corpus

To identify whether AQP5 can be a SPEM cell marker in humans, we examined tissue microarray slides composed of human normal and metaplasia gastric samples. In the normal corpus and antrum, foveolar, isthmic, or mucous neck cells were marked by UEAI, Ki67, or GSII, respectively, but intestinal epithelial markers DEFA5 and TFF3 were not present in normal oxyntic and antral glands (Figure 7*A* and *B*). Although normal oxyntic glands in the corpus did not express AQP5 and CD44v9, expression of these proteins was observed at the bases of normal antral glands along with prominent GSII positivity (Figure 7*A* and *B*). As in mice, human corpus glands with pyloric metaplasia showed SPEM cells with foamy cytoplasm as well as positivity for periodic acid-Schiff (PAS) staining, and most of the SPEM cells in all 44 cores were markedly positive for GSII and AQP5 as well as CD44v9, similar to the pattern in the deep antral gland cells of the normal antrum (Figure 7*C*). These data indicate that AQP5 is a lineage-specific marker for SPEM cells in the human corpus. In contrast, TROP2, which is associated with incomplete IM and dysplastic transition of metaplastic glands,[32] was not detected in the normal corpus, antrum, and SPEM lesions.

## TROP2 Is Predominantly Expressed in the Incomplete IM Rather Than Complete IM

As described above, IM is frequently observed in adjacent non-tumor tissue of gastric cancer patients. We therefore sought to identify a specific pattern of protein expression in IM distinct from that in SPEM. IM lesions were confirmed by H&E, PAS, and high-iron diamine/Alcian blue (HID/AB) staining and classified into 2 groups, complete or incomplete. In complete IM, mucin in the goblet cells was stained bright magenta in PAS and blue in

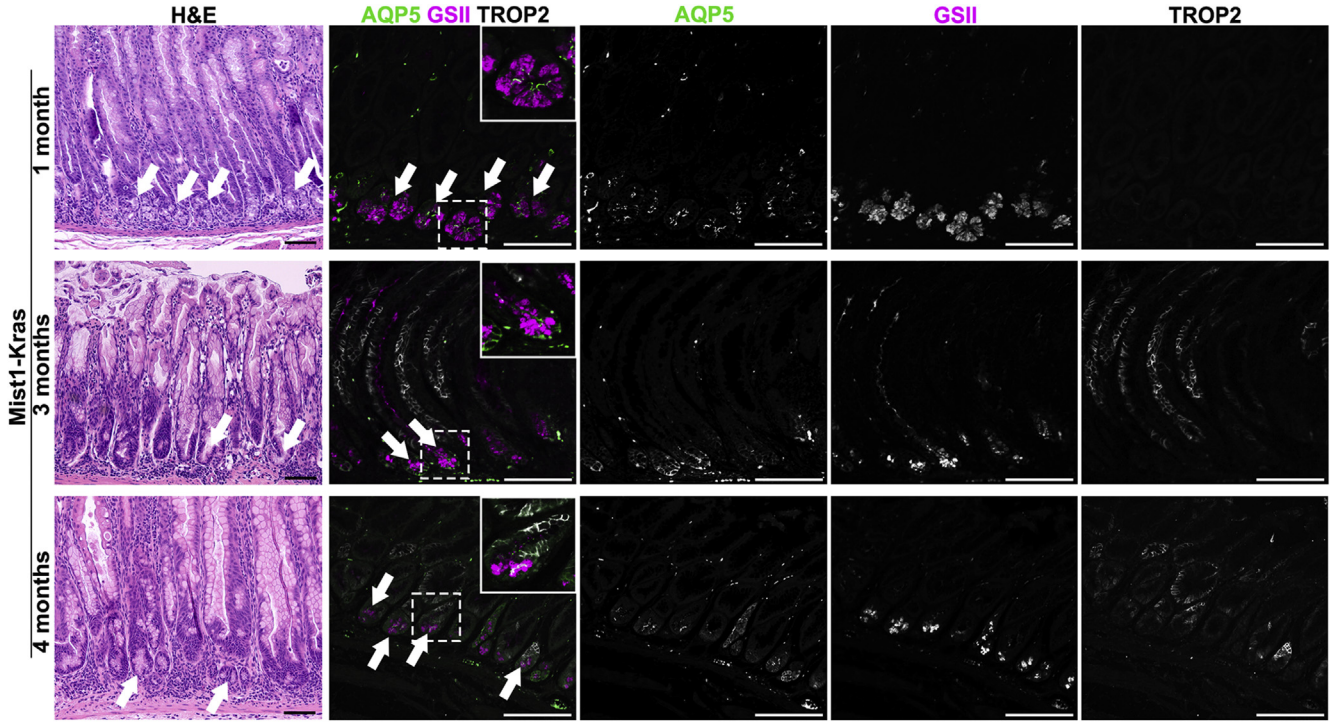


**Figure 6. AQP5 is expressed in SPEM cells induced by Kras activation in Mist1-positive chief cells.** H&E and immunofluorescence staining (IF) for AQP5, mucus marker GSII-lectin, and the dysplasia marker TROP2 in gastric corpus tissues from *Mist1*$^{CreERT2/+}$;*Kras*$^{LSL\text{-}G12D/+}$ mice. Corpus mucosa 1 month after induction by tamoxifen showed only SPEM lesions marked by AQP5 and GSII-lectin co-positivity. Three or 4 months after Kras activation in Mist1-positive cells, corpus glands were composed of AQP5- and GSII-lectin co-positive cells at the bases of glands with TROP2-expressing cells in the upper gland. *Arrows* indicate SPEM cells at the base of glands (H&E) and AQP5-expressing cells (IF). *Insets* show higher magnifications of boxed areas. No expression of AQP5 in the TROP2-positive region was noted. Scale bar = 100 $\mu$m.

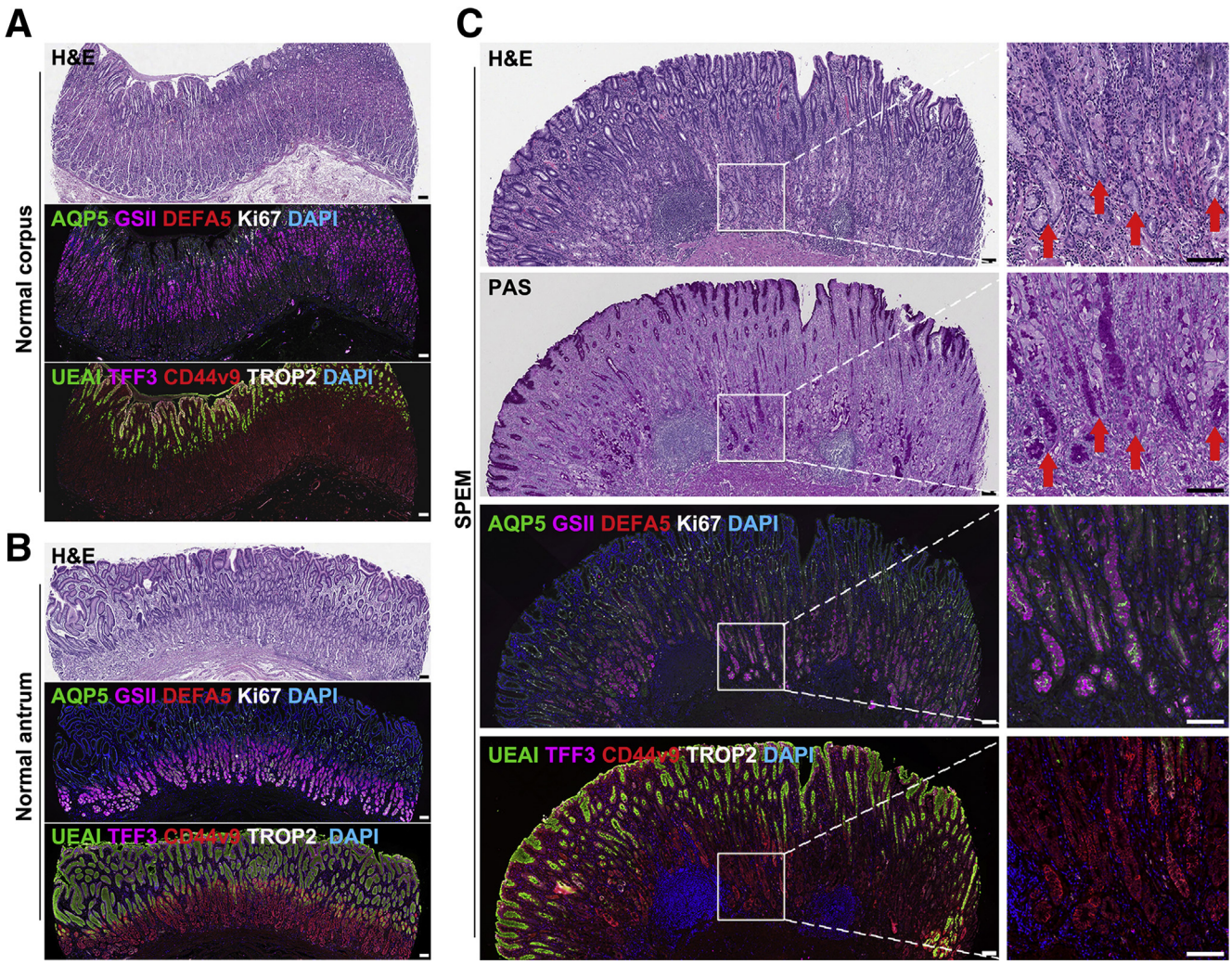


**Figure 7. AQP5 is not expressed in human normal gastric corpus but is strongly expressed in normal antrum SPEM cell lineages.** Histology and immunostaining were examined in sections of human (*A*) normal corpus, (*B*) normal antrum, and (*C*) SPEM. Sections were stained for H&E staining for identification of overall structure of normal corpus, antrum, and SPEM in the corpus, PAS staining to confirm localization of mucous accumulation in normal or SPEM lesions, and immunofluorescence staining for AQP5, mucus marker GSII-lectin, Paneth cell marker DEFA5, proliferative cell marker Ki67, foveolar cell marker *Ulex europaeus agglutinin* I (UEAI), goblet cell marker TFF3, SPEM marker CD44v9, dysplasia marker TROP2, and nuclei marker DAPI. Note that PAS-positive SPEM cell lineages (*arrows*) were marked by expression of AQP5, GSII, and CD44v9 (*C*, expanded images). Scale bar = 100 $\mu$m.

HID/AB staining with TFF3 positivity (Figure 8*A*). In addition, DEFA5-expressing Paneth cells were frequently observed only at the base of complete IM glands, similar to the pattern in intestinal crypts (Figure 8). Using immunostaining for basolateral CD44v9 expression, we confirmed that the complete type of intestinal metaplastic glands in the stomach have morphologic characteristics similar to intestine, with CD44v9-expressing cells at the bases of these glands. Nevertheless, complete IM glands lacked GSII or AQP5 expressing cells (Figure 8). Indeed, UEAI, GSII, and TROP2 were hardly ever observed in complete IM (Figure 8).

In incomplete IM, the mucin droplets in goblet cells were stained bright magenta in PAS staining and positive for TFF3, similar with that in complete IM, but mucin granule size was often smaller or variable in size (Figure 9*A*). Some areas of incomplete IM also showed brown staining indicating the presence of sulfomucins in HID/AB staining (Figure 9*A*). Furthermore, the incomplete IM glands did not have any Paneth cells marked by DEFA5 and frequently expressed TROP2 as well as CD44v9 (Figure 9).

## *AQP5 Is Expressed in Cells at the Base of Incomplete IM, but not in Complete IM*

Interestingly, most of the metaplastic tissue cores showed a full spectrum of gastric metaplasia including SPEM and IM, and these 2 distinct types of metaplasia were often intermixed. On the basis of previous work,[30,33] we sought to examine the possible relationship between

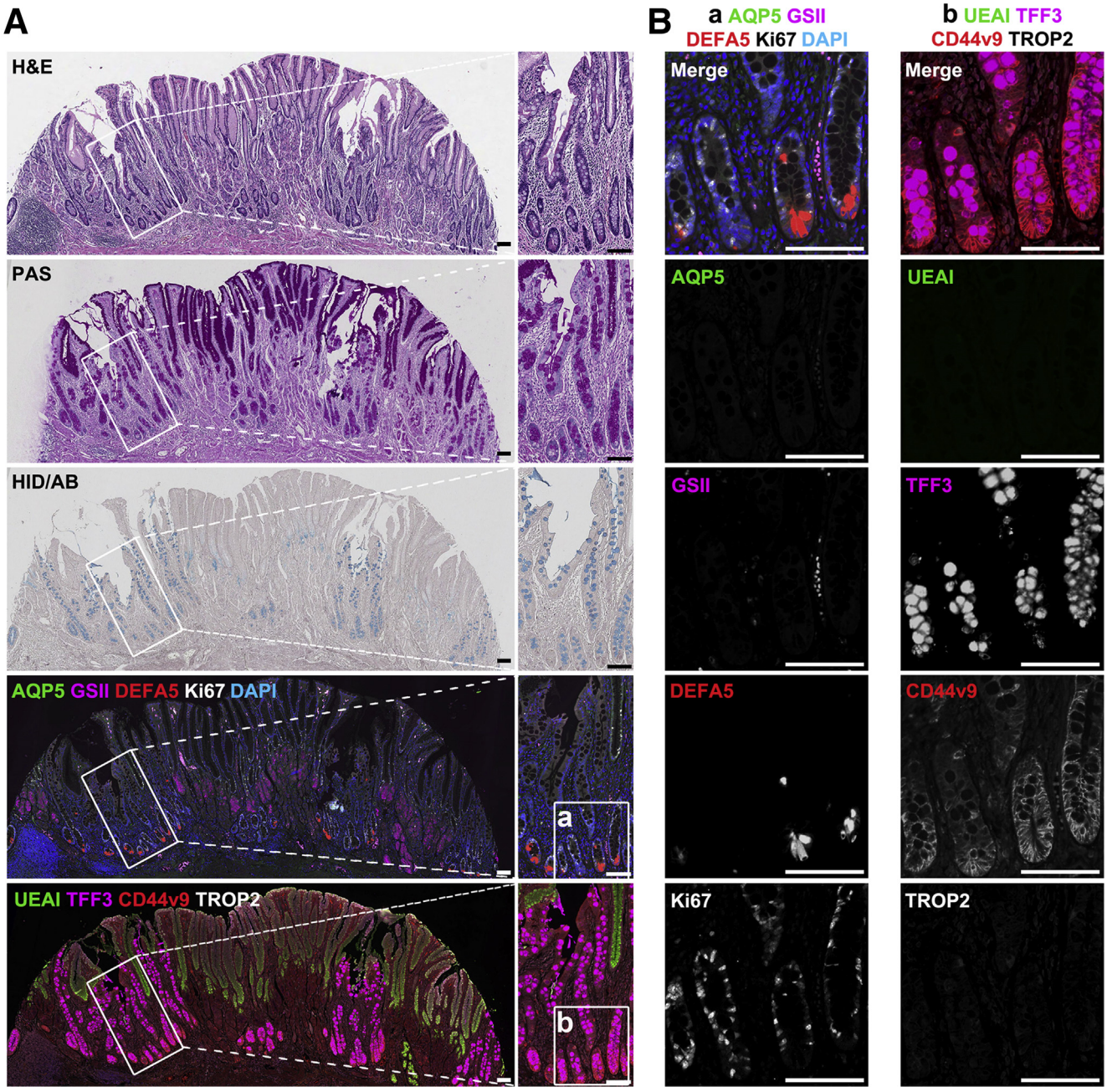


**Figure 8. AQP5 is not expressed in complete type of IM.** (*A*) H&E staining for identification of overall structure of IM in the corpus, PAS staining to confirm localization of mucous accumulation in IM lesion, HID/AB staining to determine the subtype of IM and immunofluorescence staining for AQP5, mucus marker GSII-lectin, Paneth cell marker DEFA5, proliferative cell marker Ki67, foveolar cell marker *Ulex europaeus agglutinin* I (UEAI), goblet cell marker TFF3, SPEM marker CD44v9, dysplasia marker TROP2, and nuclei marker DAPI. Complete IM glands were characterized by eosinophilic granules-containing Paneth cells (H&E) stained with DEFA5 and TFF3-positive sialomucin stained blue in HID/AB staining. CD44v9 was also expressed at the base of complete IM gland. Scale bar = 100 $\mu$m. (*B*) Expanded images from immunofluorescence staining results in (*A*). Complete IM gland had Paneth and goblet cells frequently showing basolateral CD44v9 expression and proliferative activity similar to an intestinal crypt. Note absence of TROP2 and AQP5 expression. Scale bar = 50 $\mu$m.

SPEM and IM. As shown in Figures 9 and 10, AQP5-expressing cells at the base of metaplastic glands were prominently observed in incomplete IM (61.7%) rather than in complete IM (2.6%). To directly compare AQP5-positive SPEM and TROP2 expression between complete and incomplete IM, we selected cores containing both types of IM. Consistently, incomplete IM glands contained SPEM cells, as defined by AQP5- and GSII-co-expression, at their bases with TROP2-positive cells in the upper parts of the glands (Figure 10*A* and *B*). In contrast, complete IM glands showed extremely low frequencies of AQP5 and TROP2 positivity (Figure 10*A*–*C*), rather showing DEFA5-

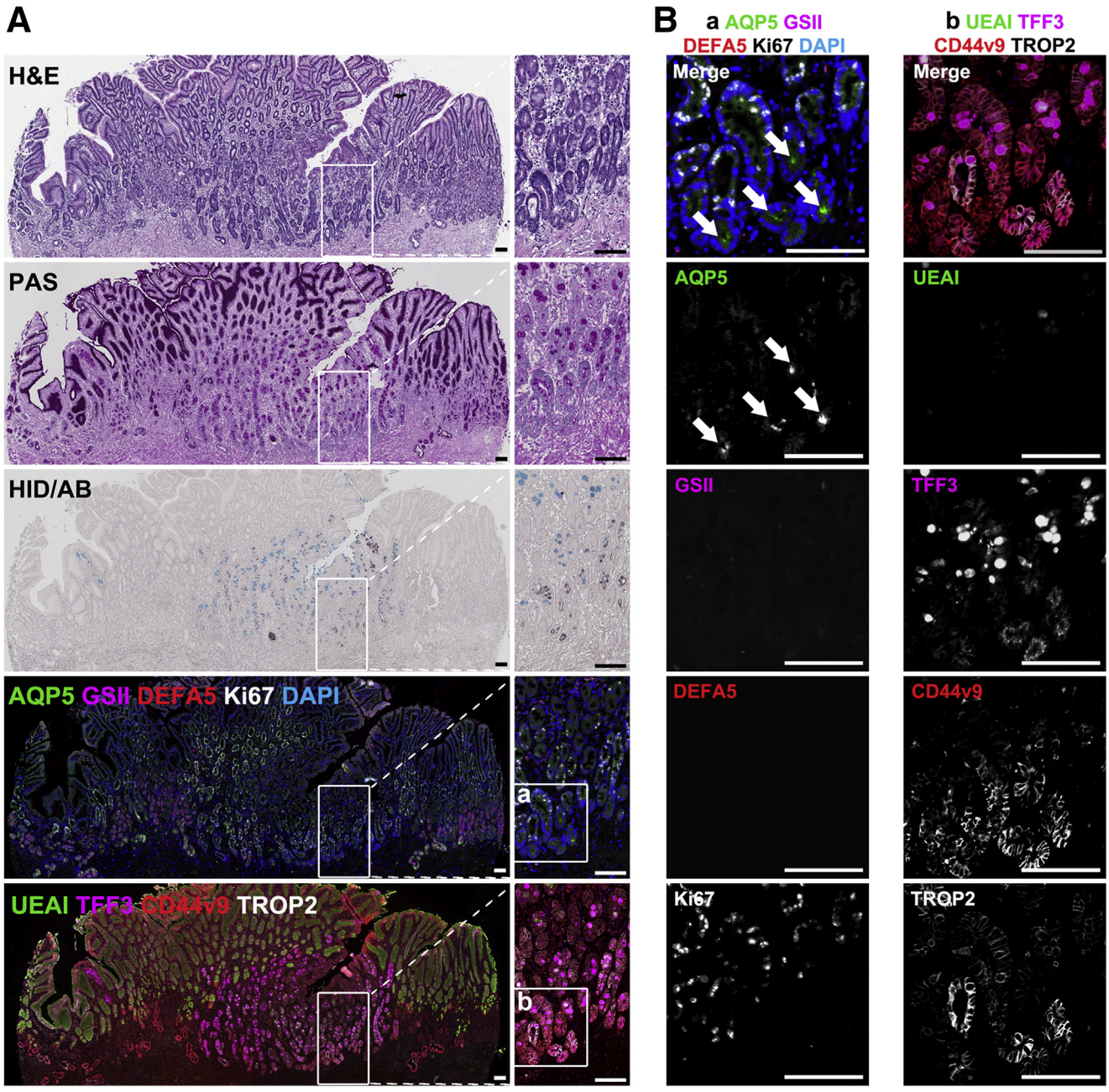


**Figure 9. AQP5-expressing cells were observed at base of incomplete IM glands showing TROP2 positivity.** (*A*) H&E staining for identification of overall structure of IM in the corpus, PAS staining to confirm localization of mucous accumulation in IM lesion, HID/AB staining to determine subtype of IM, and immunofluorescence staining for AQP5, mucus marker GSII-lectin, Paneth cell marker DEFA5, proliferative cell marker Ki67, foveolar cell marker *Ulex europaeus agglutinin* I (UEAI), goblet cell marker TFF3, SPEM marker CD44v9, dysplasia marker TROP2, and nuclei marker DAPI. Incomplete IM glands were defined on the basis of absence of DEFA5-positive Paneth cells, morphology of PAS-positive mucin, and sulfomucin stained brown in HID/AB staining. Scale bar = 100 $\mu$m. (*B*) Expanded images from immunofluorescence staining results in (*A*). Incomplete IM glands were marked by TROP2 expression. Note AQP5-expressing cells were frequently observed at base of incomplete IM glands (*arrows*). Scale bar = 50 $\mu$m.

positive Paneth cells in the basal position (Figure 8*B*). In incomplete IM glands, SPEM cells were present at the gland base below IM and TROP2-expressing cells (Figure 10*D*). To examine these correlations further, we also evaluated CD10 staining as a columnar enterocyte marker, which is present in complete IM glands (Figure 10*D*). CD10 staining was not observed in TROP2-expressing incomplete IM glands. No AQP5 staining was observed in TROP2-positive dysplastic cells. Together, these findings suggest that AQP5-expressing SPEM cells may contribute to incomplete IM glands marked by expression of TROP2.

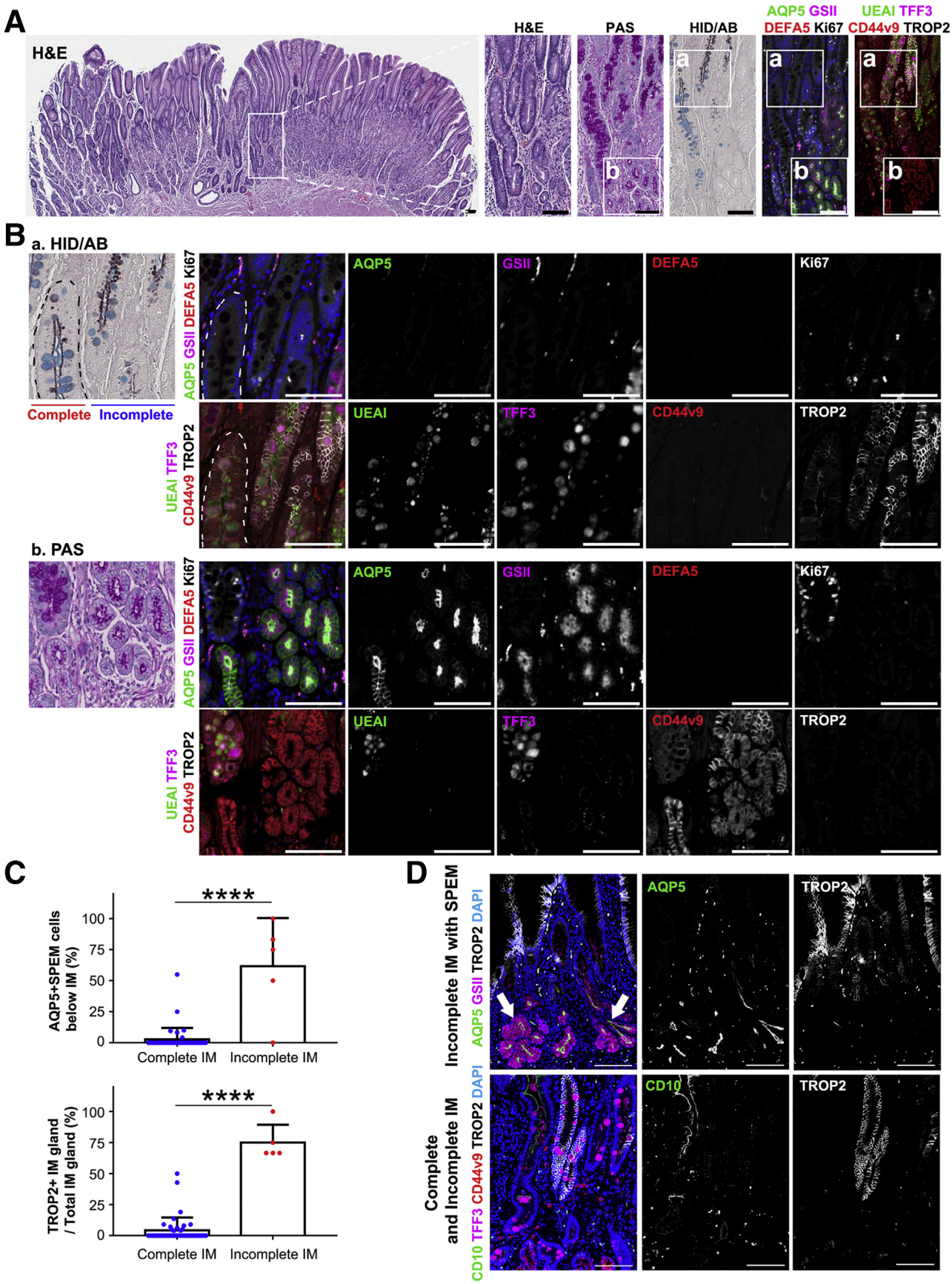
A
H&E
H&E
PAS
HID/AB
AQP5 GSII DEFA5 Ki67
UEAI TFF3 CD44v9 TROP2
a
b
B
a. HID/AB
Complete
Incomplete
AQP5 GSII DEFA5 Ki67
UEAI TFF3 CD44v9 TROP2
AQP5
GSII
DEFA5
Ki67
UEAI
TFF3
CD44v9
TROP2
b. PAS
C
AQP5+SPEM cells below IM (%)
TROP2+ IM gland / Total IM gland (%)
****
Complete IM
Incomplete IM
D
Incomplete IM with SPEM
AQP5 GSII TROP2 DAPI
Complete and Incomplete IM
CD10 TFF3 CD44v9 TROP2 DAPI
CD10

## Discussion

Intestinal-type gastric cancer usually arises within a field of precancerous metaplastic changes in the stomach mucosa. Over the past 100 years, 2 types of metaplastic lesions have been described as pyloric metaplasia/SPEM and IM.[1,34] These metaplastic lesions are frequently observed in the gastric mucosa adjacent to intestinal-type gastric cancers.[2,35–37] SPEM evolves as a first metaplasia after the induction of severe mucosal injury in the stomach corpus, predominantly through transdifferention of chief cells in mucous cell metaplasia.[8,38,39] IM appears to develop subsequently in the face of more chronic inury, often within a field of preexisting SPEM.[6,33] In addition, IM has been subclassified into incomplete versus complete types of IM. Complete IM glands demonstrate well-developed MUC2/TFF3-positive goblet cells along with CD10-positive absorptive intestinal cells and DEFA5-positive Paneth cells. In contrast, incomplete IM glands show immature goblet cells and intermediate columnar cells with mucin droplets that may contain gastric and/or intestinal mucins (sialomucins and/or sulfomucin), and the glands lack absorptive or Paneth cell lineages. Importantly, incomplete IM carries a far higher risk of patient progression to gastric adenocarcinoma compared with complete IM.[40,41] Nevertheless, all of these metaplastic lineages are often present in a field of preneoplastic mucosa in the stomach, so development of more sophisticated markers that can distinguish among metaplasia types remains a priority. In the present study, we have demonstrated that AQP5, which was recently identified in the deep antral gland mucous cells,[22] is also a specific marker for SPEM cells in the corpus in both mouse SPEM models and human metaplasia samples. Furthermore, we have identified a likely link of SPEM cells with incomplete IM through AQP5 staining at the bases of these preneoplastic glands.

Since SPEM was first reported in 1999,[5] the morphologic characteristics and etiology of SPEM cells have been elucidated by several groups through work in mouse models and human tissue.[10,42–44] SPEM cells express TFF2 and MUC6/GSII, and recent studies showed that CD44v9, a splice variant of the cell surface glycoprotein CD44, is prominently expressed in SPEM cells.[6,37,45] However, making a diagnosis using a single marker might be confusing because these proteins are also expressed in other types of cells or lesions; TFF2 and MUC6/GSII are expressed in normal mucous neck cells in the corpus, and CD44v9 can be expressed in proliferating cells and IM lesions.[46] However, in this study we determined that AQP5 specifically defines a SPEM cell lineage in the corpus without expression in complete IM. Recent articles proposed a new term *paligenosis* describing a regenerative process of fully differentiated cells.[47–49] Our data also indicate that chief cells undergoing transdifferentiation or "paligenosis" variably express AQP5 during progression to SPEM cell or returning to normal chief cell. Etiologically in humans, SPEM begins with sustained inflammation and oxyntic atrophy, or parietal cell loss, related to *H pylori* infection. We and others have used drug-induced mouse SPEM models to model human SPEM through induction of acute parietal cell loss.[5,8,42] It was also reported that SPEM development can be induced by Epstein-Barr virus.[35] Our previous studies revealed a role of host immune response and IL13 released from innate lymphoid cell populations (ILC2s) in the initiation of SPEM development.[28,29] Our present findings demonstrate that AQP5 is up-regulated early in transdifferentiating chief cells after the induction of oxyntic atrophy and ILC2-mediated release of IL13. We have previously noted that a lack of xCT expression led to an arrest of transdifferentiation at a stage after the down-regulation of Mist1 expression.[24] Because xCT deletion did not alter the up-regulation of AQP5 expression in transdifferentiating chief cells, AQP5 up-regulation also represents a very early step in the transdifferentiation process for chief cells. Importantly, AQP5 expression is sustained in SPEM observed in chronic *H felis* infection in mice and in human SPEM samples. All of these results suggest that AQP5 is uniquely up-regulated during the process of transdifferentiation of chief cells into SPEM, but AQP5 expression is lost during progression of lesions toward intestinalized lineages. AQP5 expression in basal gland cells in combination with Trop2 positivity in more luminal intestinal lineages therefore defines the state of lineage confusion within incomplete IM that can lead to dysplasia.

Aquaporins promote bidirectional transfer of water and small molecules in epithelial cells.[16,50] In particular, AQP5

**Figure 10.** (***See previous page***). **Incomplete IM glands within regions mixed IM types demonstrate AQP5-expressing cells at the base.** H&E staining for identification of overall structure of the IM in the corpus, PAS staining to confirm localization and morphology of mucus in IM lesion, HID/AB staining to determine subtype of IM, and immunofluorescence staining for AQP5, mucus marker GSII-lectin, Paneth cell marker DEFA5, proliferative cell marker Ki67, foveolar cell marker *Ulex europaeus agglutinin* I (UEAI), goblet cell marker TFF3, SPEM marker CD44v9, dysplasia marker TROP2, and nuclei marker DAPI. Differentiation of IM subtype was determined on the basis of combination of H&E, PAS, and HID/AB staining results as described in Figures 6 and 7. Scale bar = 100 $\mu$m. (*B*) Expanded images from PAS and HID/AB staining results in (*A*) with matched immunofluorescence images. Gland delineated by *dotted line* indicates complete IM gland, and others are incomplete IM glands. TROP2 was strongly expressed in incomplete IM gland, which showed cells at the base with CD44v9 positivity and strong AQP5 expression. Scale bar = 50 $\mu$m. (*C*) Quantification of individual IM glands in corpus accompanied by AQP5-positive cells at base of the gland per each core (n = 44 for complete IM and 5 for incomplete IM; *top*) or quantification of individual IM glands with TROP2 expression per each core (n = 44 of complete IM and 5 of incomplete IM; *bottom*) ****$P < .0001$. (*D*) Immunofluorescence staining for AQP5, GSII-lectin, TROP2, intestinal absorptive cell marker CD10, TFF3, CD44v9, and DAPI in whole tissue sections from human metaplasia tissues. AQP5- and GSII-lectin co-positive SPEM below TROP2-expressing incomplete IM (*top*) and CD10-negative and TROP2-positive incomplete IM gland (*bottom*). Note basal branched glands populated with SPEM cells (*arrows*). Scale bar = 100 $\mu$m.

can also promote cell viability by enhancing cell cycle progression and inhibiting apoptosis.[51,52] A recent study reported that AQP5 in human and mouse is essential for maintaining antral stem cell function and is highly expressed in gastric cancers in the antrum.[22] These functions of AQP5 might be associated with the initiation of transdifferentiation for chief cells; however, it is not clear whether AQP5 is required for development of SPEM at this time. Nevertheless, the staining of AQP5 represents a critical marker of pyloric metaplastic glands in the corpus of the stomach. Because pyloric metaplasia represents a prominent mechanism for repair of severe mucosal injury throughout the gastrointestinal tract,[53] further investigations are needed to define whether AQP5 up-regulation is also involved in other examples of pyloric metaplasia.

IM is considered a prevalent precancerous lesion in stomach, which manifested in 2 types of glands with complete or incomplete IM.[40,54,55] Patients with IM in the corpus or incomplete IM have a higher risk of gastric cancer compared with patients demonstrating IM confined to the antrum or complete IM.[33,40,41] Several methods have been used to classify complete and incomplete IM, including H&E, PAS, or HID/AB staining. However, these techniques may not be sufficient to delineate heterogeneity in metaplastic lesions. In addition, the HID staining process is quite toxic. Our present study defines metaplastic gland phenotypes that are based on immunostaining markers for multiple cell lineages. Although normal corpus glands lack AQP5 expression, our investigations showed that SPEM cell lineages prominently expressed the protein at the apical membrane. Just as interestingly, we also saw AQP5-expressing lineages at the bases of glands that expressed Trop2 and TFF3 in their upper regions, consistent with identification of incomplete IM. In the present study and previous work,[31] we found that Trop2 was up-regulated in incomplete IM, but not in complete IM. Similarly, no AQP5 staining was observed in complete IM, although CD44v9 positive cells could be observed at the bases of these complete IM glands. These findings suggest that SPEM cells are often present at the bases of glands with incomplete IM.

Interestingly, we observed AQP5 and GSII dual positive SPEM cells at the bases of IM and dysplastic glands, which also showed more luminal Trop2-positive cells, in Mist1-Kras mice at 3 and 4 months after induction of Kras. These findings would suggest that the metaplasia in these mice is also consistent with an incomplete IM phenotype. In a previous study, we observed that treatment of Mist1-Kras mice 3 months after induction with a MEK inhibitor elicited an up-regulation of apical villin expression, which is consistent with differentiation toward absorptive enterocytes, a characteristic of complete IM.[56] These results would therefore be compatible with a scenario where oxyntic atrophy initially induces SPEM, which can then give rise to incomplete IM. However, under influences that would promote reduction in Kras activation, then glands could evolve to complete IM. Under this paradigm, because incomplete IM represents the more carcinogenic scenario in the stomach, maintenance of Ras activation represents a critical drive for evolution of dysplasia and gastric adenocarcinoma. Nevertheless, it remains possible that multiple scenarios exist for the evolution of metaplastic cell lineages in the stomach. Specimens could be identified with SPEM directly associated with TROP2-expressing dysplasia without evidence of IM.[32] Thus, we cannot rule out the possibility that SPEM could directly give rise to dysplasia. Similarly, we cannot rule out the possibility that SPEM could give rise to complete IM directly.

In summary, we have described the utility of AQP5 as a marker of SPEM cells in both mice and humans. AQP5 expression is lost in complete IM glands, but a nidus of AQP5-expressing SPEM cells is usually present at the bases of incomplete IM glands. The combination of immunostaining for AQP5, Trop2, CD44v9, and TFF3 can therefore rapidly define the range of lineages present in the metaplastic stomach of human patients. Metaplastic lesions in stomach are known to be unequivocally associated with intestinal-type gastric cancer; however, the reversibility of these lesions remains controversial. Because of the focal nature of incomplete metaplastic glands in the stomach corpus, this combination of lineage-specific markers may assist in better defining how metaplasias develop and progress and could assist with therapeutic strategies to assess precancerous lesions and determine more accurately those at highest risk for gastric carcinogenesis.

# Methods

## Experimental Animal Models

The care, maintenance, and treatment of mice used in this study followed protocols approved by the Institutional Animal Care and Use Committee of Vanderbilt University Medical Center, and each experimental group contained 3–6 mice. Littermates from both sexes were randomly assigned to experimental groups. Mice were maintained in housing of 5 animals per cage, with a 12-hour light/dark cycle and water and food at libitum. Mouse models and treatment of mice were described previously.[24,28,30,57] C57BL/6 mice were orally injected with L-635 (350 mg/kg per day) once and then allowed to have a recovery time for 2 or 4 days or injected with same concentration of L-635 once a day for 1, 2, or 3 days or DMP-777 (350 mg/kg per day) once daily for 1, 3, 7, or 14 days. C57BL/6 mice were subjected to 100% of acetic acid-induced localized gastric injury as described previously.[58] As a chronic SPEM model, C57BL/6 mice were orally infected with *H felis* in 500 $\mu$L of bacterial cell suspension ($1 \times 10^9$ units/mL) every other day total 3 times. The $Mist1^{CreERT2/+};Kras^{LSL\text{-}G12D/+}$ mice were subcutaneously injected with 5 mg tamoxifen for 3 consecutive days at 8 weeks of age.

## Human IM Arrays

Human gastric array sets for IM/SPEM were constructed with specimens from 18 patients (age, 39–81 years) who underwent surgical resection for gastric cancers in Jeju National University Hospital from 2014 to 2020 in Korea. Through histologic examination, IM or SPEM areas were

**Table 1.** List of Primary Antibodies and Fluorescent Dye-Conjugated Lectins

| Antibody | Species | Source | Dilution |
|---|---|---|---|
| CD44v9 for mouse | Rat | Cosmo Bio, LKG-M002 | 1:25,000 |
| CD44v9 for human | Rat | Cosmo Bio, LKG-M001 | 1:15,000 |
| AQP5 | Rabbit | Sigma-Aldrich, HPA065008 | 1:500 |
| TFF3 | Rabbit | Gift from Daniel K. Podolsky (UT Southwestern) | 1:1000 |
| Trop2 for mouse | Goat | R&D Systems, AF1122 | 1:500 |
| TROP2 for human | Goat | R&D Systems, AF650 | 1:500 |
| MUC5AC | Mouse | NeoMarkers, MS-551-P | 1:500 |
| DEFA5 | Mouse | Santa Cruz, sc-53997 | 1:1000 |
| Ki67 | Rat | LS Bio, LS-C338537 | 1:150 |
| P120 | Mouse | BD Biosciences, 610133 | 1:100 |
| GIF | Goat | Santa Cruz, sc-46656 | 1:500 |
| GSII lectin, Alexa Fluor 647 conjugated | | Molecular probes, L32451 | 1:2000 |
| UEAI, FITC conjugated | | Sigma-Aldrich, L9006 | 1:2000 |
| CD10, Alexa Fluor 488 conjugated | | Santa Cruz, sc-46656 | 1:50 |

selected from H&E-stained slides. The tissue cores of 4 mm in diameter were obtained from individual paraffin blocks and arranged in a new recipient paraffin block using a trephine apparatus (SuperBioChips Laboratories, Seoul, Korea). In total, 4 tissue arrays were generated: IM or SPEM in the corpus (n = 48), IM in the antrum (n = 30), normal corpus (n = 9), and normal antrum (n = 9). Tissue array construction was approved by the Institutional Review Board of Jeju National University Hospital (2016-10-001), and informed consent was waived by the Institutional Review Board because of the retrospective nature of the study.

## Immunostaining

Five-micrometer paraffin-embedded tissue sections were deparaffinized in Histoclear and rehydrated through a series of ethanol (100%, 95%, 75%). Antigen retrieval was performed using Dako (Glostrup, Denmark) Target retrieval solution, pH 6, in a pressure cooker for 15 minutes. Tissue sections were incubated in Dako Serum-free Protein Block Solution at room temperature for 90 minutes, and primary antibodies were applied overnight at 4°C (Table 1). The following day, tissue slides were washed in phosphate-buffered saline for 5 minutes 3 times. Secondary antibodies were applied to the tissue sections at room temperature for 60 minutes. Nuclei counterstaining was performed using Hoechst or diamidino-2-phenylindol (DAPI) in phosphate-buffered saline for 5 minutes at room temperature. All immunofluorescence images of mouse or human stomach tissues were captured with a Zeiss Axio Imager 2 (Oberkochen, Germany) using a ×20 objective or Leica Aperio Versa 200 Fluorescent Slide Scanner in the Vanderbilt Digital Histology Shared Resource, respectively.

## HID/AB Staining

As previously published,[59] tissue sections were deparaffinized and rehydrated in distilled water, rinsed in running tap water for 5 minutes, and then placed in freshly prepared HID solution using plastic racks. The HID was prepared by dissolving simultaneously 2 amines (N,N-dimethyl-m-phenylenediamine dihydrochloride [Sigma-Aldrich, St Louis, MO], 0.720 g and N,N-dimethyl-p-phenylenediamine monohydrochloride, Grade II, [Sigma-Aldrich], 0.120 g) in 300 mL of distilled water and then pouring this solution into a staining dish containing 8.4 mL of 62% ferric chloride solution. The pH was controlled between 1.3 and 1.7. The tissue sections were maintained in this solution in the dark at room temperature for 18–24 hours. Then they were rinsed in and out with distilled water and stained in 1% Alcian blue solution (Alcian blue 8GX [Sigma-Aldrich] and 3% acetic acid solution) for 30 minutes, filtering the solution before use. The tissue sections were rinsed again in and out with distilled water, dehydrated in 95% alcohol and absolute alcohol, 2 changes each, cleared in xylene, 2 changes, and mounted with Permount.

## IM Subtyping

IM was classified as complete or incomplete types by combined assessment of H&E, PAS, and HID/AB stains in each tissue core. The presence of more than one IM type was annotated.

## Data Analysis

Three or 4 representative images were obtained from each mouse, and then positivity of each lineage-specific marker was manually quantitated per gland. In 48 cores of human metaplasia tissues, 39 cores had only complete type IM, and 5 cores had both complete and incomplete IM. Among total TFF3-positive glands in complete or incomplete IM, frequency of specific marker, TROP2 or AQP5, expression was manually counted per gland. All statistical analyses were generated using unpaired Student *t* test in GraphPad Prism 7 software (La Jolla, CA).

## References


1. Jencks DS, Adam JD, Borum ML, Koh JM, Stephen S, Doman DB. Overview of current concepts in gastric intestinal metaplasia and gastric cancer. Gastroenterol Hepatol (N Y) 2018;14:92–101.
2. Goldenring JR. Pyloric metaplasia, pseudopyloric metaplasia, ulcer-associated cell lineage and spasmolytic polypeptide-expressing metaplasia: reparative lineages in the gastrointestinal mucosa. J Pathol 2018; 245:132–137.
3. Que J, Garman KS, Souza RF, Spechler SJ. Pathogenesis and cells of origin of Barrett's esophagus. Gastroenterology 2019;157:349–364 e1.
4. Jin RU, Mills JC. Are gastric and esophageal metaplasia relatives? the case for Barrett's stemming from SPEM. Dig Dis Sci 2018;63:2028–2041.
5. Schmidt PH, Lee JR, Joshi V, Playford RJ, Poulsom R, Wright NA, Goldenring JR. Identification of a metaplastic cell lineage associated with human gastric adenocarcinoma. Lab Invest 1999;79:639–646.
6. Yoshizawa N, Takenaka Y, Yamaguchi H, Tetsuya T, Tanaka H, Tatematsu M, Nomura S, Goldenring JR, Kaminishi M. Emergence of spasmolytic polypeptide-expressing metaplasia in Mongolian gerbils infected with Helicobacter pylori. Lab Invest 2007;87:1265–1276.
7. Meyer AR, Goldenring JR. Injury, repair, inflammation and metaplasia in the stomach. J Physiol 2018; 596:3861–3867.
8. Nam KT, Lee HJ, Sousa JF, Weis VG, O'Neal RL, Finke PE, Romero-Gallo J, Shi G, Mills JC, Peek RM, Konieczny SF, Goldenring JR. Mature chief cells are cryptic progenitors for metaplasia in the stomach. Gastroenterology 2010;139:2028–2037.
9. Stange DE, Koo BK, Huch M, Sibbel G, Basak O, Lyubimova A, Kujala P, Bartfeld S, Koster J, Geahlen JH, Peters PJ, van Es JH, van de Wetering M, Mills JC, Clevers H. Differentiated Troy+ chief cells act as reserve stem cells to generate all lineages of the stomach epithelium. Cell 2013;155:357–368.
10. Nam KT, Lee HJ, Mok H, Romero-Gallo J, Crowe JE Jr, Peek RM Jr, Goldenring JR. Amphiregulin-deficient mice develop spasmolytic polypeptide expressing metaplasia and intestinal metaplasia. Gastroenterology 2009; 136:1288–1296.
11. Petersen CP, Weis VG, Nam KT, Sousa JF, Fingleton B, Goldenring JR. Macrophages promote progression of spasmolytic polypeptide-expressing metaplasia after acute loss of parietal cells. Gastroenterology 2014; 146:1727–1738 e8.
12. Shah SC, Gawron AJ, Mustafa RA, Piazuelo MB. Histologic subtyping of gastric intestinal metaplasia: overview and considerations for clinical practice. Gastroenterology 2020;158:745–750.
13. Choi BH, Pagano M, Dai W. Plk1 protein phosphorylates phosphatase and tensin homolog (PTEN) and regulates its mitotic activity during the cell cycle. J Biol Chem 2014;289:14066–14074.
14. Fushimi K, Uchida S, Hara Y, Hirata Y, Marumo F, Sasaki S. Cloning and expression of apical membrane water channel of rat kidney collecting tubule. Nature 1993;361:549–552.
15. Knepper MA. The aquaporin family of molecular water channels. Proc Natl Acad Sci U S A 1994;91:6255–6258.
16. Direito I, Madeira A, Brito MA, Soveral G. Aquaporin-5: from structure to function and dysfunction in cancer. Cell Mol Life Sci 2016;73:1623–1640.
17. Wang KS, Komar AR, Ma T, Filiz F, McLeroy J, Hoda K, Verkman AS, Bastidas JA. Gastric acid secretion in aquaporin-4 knockout mice. Am J Physiol Gastrointest Liver Physiol 2000;279:G448–G453.
18. Fukuhara S, Matsuzaki J, Tsugawa H, Masaoka T, Miyoshi S, Mori H, Fukushima Y, Yasui M, Kanai T, Suzuki H. Mucosal expression of aquaporin-4 in the stomach of histamine type 2 receptor knockout mice and Helicobacter pylori-infected mice. J Gastroenterol Hepatol 2014;29(Suppl 4):53–59.
19. Zhao H, Yang X, Zhou Y, Zhang W, Wang Y, Wen J, Zhang Z, Shen L. Potential role of aquaporin 3 in gastric intestinal metaplasia. Oncotarget 2015;6:38926–38933.
20. Chen J, Wang T, Zhou YC, Gao F, Zhang ZH, Xu H, Wang SL, Shen LZ. Aquaporin 3 promotes epithelial-mesenchymal transition in gastric cancer. J Exp Clin Cancer Res 2014;33:38.
21. Parvin MN, Tsumura K, Akamatsu T, Kanamori N, Hosoi K. Expression and localization of AQP5 in the stomach and duodenum of the rat. Biochim Biophys Acta 2002;1542:116–124.
22. Tan SH, Swathi Y, Tan S, Goh J, Seishima R, Murakami K, Oshima M, Tsuji T, Phuah P, Tan LT, Wong E, Fatehullah A, Sheng T, Ho SWT, Grabsch HI, Srivastava S, Teh M, Denil S, Mustafah S, Tan P, Shabbir A, So J, Yeoh KG, Barker N. AQP5 enriches for stem cells and cancer origins in the distal stomach. Nature 2020;578:437–443.
23. Lee HJ, Nam KT, Park HS, Kim MA, Lafleur BJ, Aburatani H, Yang HK, Kim WH, Goldenring JR. Gene expression profiling of metaplastic lineages identifies CDH17 as a prognostic marker in early stage gastric cancer. Gastroenterology 2010;139:213–225 e3.
24. Meyer AR, Engevik AC, Willet SG, Williams JA, Zou Y, Massion PP, Mills JC, Choi E, Goldenring JR. Cystine/glutamate antiporter (xCT) is required for chief cell plasticity after gastric injury. Cell Mol Gastroenterol Hepatol 2019;8:379–405.
25. Goldenring JR, Ray GS, Coffey RJ, Meunier PC, Haley PJ, Barnes TB, Car BD. Reversible drug-induced oxyntic atrophy in rats. Gastroenterology 2000; 118:1080–1093.
26. Nomura S, Yamaguchi H, Ogawa M, Wang TC, Lee JR, Goldenring JR. Alterations in gastric mucosal lineages induced by acute oxyntic atrophy in wild-type and gastrin-deficient mice. Am J Physiol Gastrointest Liver Physiol 2005;288:G362–G375.
27. Bertaux-Skeirik N, Wunderlich M, Teal E, Chakrabarti J, Biesiada J, Mahe M, Sundaram N, Gabre J, Hawkins J, Jian G, Engevik AC, Yang L, Wang J, Goldenring JR, Qualls JE, Medvedovic M, Helmrath MA, Diwan T, Mulloy JC, Zavros Y. CD44 variant isoform 9 emerges in response to injury and contributes to the

regeneration of the gastric epithelium. J Pathol 2017; 242:463–475.
28. Petersen CP, Meyer AR, De Salvo C, Choi E, Schlegel C, Petersen A, Engevik AC, Prasad N, Levy SE, Peebles RS, Pizarro TT, Goldenring JR. A signalling cascade of IL-33 to IL-13 regulates metaplasia in the mouse stomach. Gut 2018;67:805–817.
29. Meyer AR, Engevik AC, Madorsky T, Belmont E, Stier MT, Norlander AE, Pilkinton MA, McDonnell WJ, Weis JA, Jang B, Mallal SA, Peebles RS Jr, Goldenring JR. Group 2 innate lymphoid cells coordinate damage response in the stomach. Gastroenterology 2020;159:2077–2091 e8.
30. Choi E, Hendley AM, Bailey JM, Leach SD, Goldenring JR. Expression of activated Ras in gastric chief cells of mice leads to the full spectrum of metaplastic lineage transitions. Gastroenterology 2016; 150:918–930 e13.
31. Riera KM, Jang B, Min J, Roland JT, Yang Q, Fesmire WT, Camilleri-Broet S, Ferri L, Kim WH, Choi E, Goldenring JR. Trop2 is upregulated in the transition to dysplasia in the metaplastic gastric mucosa. J Pathol 2020;251:336–347.
32. Riera KM, Jang B, Min J, Roland JT, Yang Q, Fesmire WT, Camilleri-Broet S, Ferri L, Kim WH, Choi E, Goldenring JR. Trop2 is upregulated in the transition to dysplasia in the metaplastic gastric mucosa. J Pathol 2020;251:336–347.
33. Goldenring JR, Nam KT, Wang TC, Mills JC, Wright NA. Spasmolytic polypeptide-expressing metaplasia and intestinal metaplasia: time for reevaluation of metaplasias and the origins of gastric cancer. Gastroenterology 2010; 138:2207–2210 e1.
34. Goldenring JR, Nam KT. Oxyntic atrophy, metaplasia, and gastric cancer. Prog Mol Biol Transl Sci 2010; 96:117–131.
35. Zhang Y, Chen JN, Dong M, Zhang ZG, Zhang YW, Wu JY, Du H, Li HG, Huang Y, Shao CK. Clinical significance of spasmolytic polypeptide-expressing metaplasia and intestinal metaplasia in Epstein-Barr virus-associated and Epstein-Barr virus-negative gastric cancer. Hum Pathol 2017;63:128–138.
36. Graham DY, Rugge M, Genta RM. Diagnosis: gastric intestinal metaplasia—what to do next? Curr Opin Gastroenterol 2019;35:535–543.
37. Weis VG, Goldenring JR. Current understanding of SPEM and its standing in the preneoplastic process. Gastric Cancer 2009;12:189–197.
38. Petersen CP, Mills JC, Goldenring JR. Murine models of gastric corpus preneoplasia. Cell Mol Gastroenterol Hepatol 2017;3:11–26.
39. Mills JC, Goldenring JR. Metaplasia in the stomach arises from gastric chief cells. Cell Mol Gastroenterol Hepatol 2017;4:85–88.
40. Shao L, Li P, Ye J, Chen J, Han Y, Cai J, Lu X. Risk of gastric cancer among patients with gastric intestinal metaplasia. Int J Cancer 2018;143:1671–1677.
41. Piazuelo MB, Bravo LE, Mera RM, Camargo MC, Bravo JC, Delgado AG, Washington MK, Rosero A, Garcia LS, Realpe JL, Cifuentes SP, Morgan DR, Peek RM Jr, Correa P, Wilson KT. The Colombian chemoprevention trial: 20-year follow-up of a cohort of patients with gastric precancerous lesions. Gastroenterology 2020.
42. Nam KT, Varro A, Coffey RJ, Goldenring JR. Potentiation of oxyntic atrophy-induced gastric metaplasia in amphiregulin-deficient mice. Gastroenterology 2007; 132:1804–1819.
43. Serizawa T, Hirata Y, Hayakawa Y, Suzuki N, Sakitani K, Hikiba Y, Ihara S, Kinoshita H, Nakagawa H, Tateishi K, Koike K. Gastric metaplasia induced by Helicobacter pylori is associated with enhanced SOX9 expression via interleukin-1 signaling. Infect Immun 2016;84:562–572.
44. Sousa JF, Nam KT, Petersen CP, Lee HJ, Yang HK, Kim WH, Goldenring JR. miR-30-HNF4gamma and miR-194-NR2F2 regulatory networks contribute to the upregulation of metaplasia markers in the stomach. Gut 2016; 65:914–924.
45. Khurana SS, Riehl TE, Moore BD, Fassan M, Rugge M, Romero-Gallo J, Noto J, Peek RM Jr, Stenson WF, Mills JC. The hyaluronic acid receptor CD44 coordinates normal and metaplastic gastric epithelial progenitor cell proliferation. J Biol Chem 2013;288:16085–16097.
46. Krishnan V, Lim DXE, Hoang PM, Srivastava S, Matsuo J, Huang KK, Zhu F, Ho KY, So JBY, Khor C, Tsao S, Teh M, Fock KM, Ang TL, Jeyasekharan AD, Tan P, Yeoh KG, Ito Y. DNA damage signalling as an anticancer barrier in gastric intestinal metaplasia. Gut 2020;69:1738–1749.
47. Willet SG, Lewis MA, Miao ZF, Liu D, Radyk MD, Cunningham RL, Burclaff J, Sibbel G, Lo HG, Blanc V, Davidson NO, Wang ZN, Mills JC. Regenerative proliferation of differentiated cells by mTORC1-dependent paligenosis. EMBO J 2018;37.
48. Bockerstett KA, Lewis SA, Noto CN, Ford EL, Saenz JB, Jackson NM, Ahn TH, Mills JC, DiPaolo RJ. Single-cell transcriptional analyses identify lineage-specific epithelial responses to inflammation and metaplastic development in the gastric corpus. Gastroenterology 2020; 159:2116–2129 e4.
49. Miao ZF, Lewis MA, Cho CJ, Adkins-Threats M, Park D, Brown JW, Sun JX, Burclaff JR, Kennedy S, Lu J, Mahar M, Vietor I, Huber LA, Davidson NO, Cavalli V, Rubin DC, Wang ZN, Mills JC. A dedicated evolutionarily conserved molecular network licenses differentiated cells to return to the cell cycle. Dev Cell 2020;55:178–194 e7.
50. Nejsum LN, Kwon TH, Jensen UB, Fumagalli O, Frokiaer J, Krane CM, Menon AG, King LS, Agre PC, Nielsen S. Functional requirement of aquaporin-5 in plasma membranes of sweat glands. Proc Natl Acad Sci U S A 2002;99:511–516.
51. Shimizu H, Shiozaki A, Ichikawa D, Fujiwara H, Konishi H, Ishii H, Komatsu S, Kubota T, Okamoto K, Kishimoto M, Otsuji E. The expression and role of aquaporin 5 in esophageal squamous cell carcinoma. J Gastroenterol 2014;49:655–666.
52. Jung HJ, Park JY, Jeon HS, Kwon TH. Aquaporin-5: a marker protein for proliferation and migration of human breast cancer cells. PLoS One 2011;6:e28492.
53. Kolev HM, Tian Y, Kim MS, Leu NA, Adams-Tzivelekidis S, Lengner CJ, Li N, Kaestner KH. A FoxL1-

CreERT-2A-tdTomato mouse labels subepithelial telocytes. Cell Mol Gastroenterol Hepatol 2021.
54. Correa P, Piazuelo MB, Wilson KT. Pathology of gastric intestinal metaplasia: clinical implications. Am J Gastroenterol 2010;105:493–498.
55. Dhingra R, Natov NS, Daaboul Y, Guelrud M, Cherukara A, Hung PF, Sterling MJ. Increased risk of progression to gastric adenocarcinoma in patients with non-dysplastic gastric intestinal metaplasia versus a control population. Dig Dis Sci 2020;65:3316–3323.
56. Yang Q, Yasuda T, Choi E, Toyoda T, Roland JT, Uchida E, Yoshida H, Seto Y, Goldenring JR, Nomura S. MEK inhibitor reverses metaplasia and allows re-emergence of normal lineages in Helicobacter pylori-infected gerbils. Gastroenterology 2019;156:577–581 e4.
57. Choi E, Petersen CP, Lapierre LA, Williams JA, Weis VG, Goldenring JR, Nam KT. Dynamic expansion of gastric mucosal doublecortin-like kinase 1-expressing cells in response to parietal cell loss is regulated by gastrin. Am J Pathol 2015;185:2219–2231.
58. Okabe S, Amagase K. An overview of acetic acid ulcer models: the history and state of the art of peptic ulcer research. Biol Pharm Bull 2005;28:1321–1341.
59. Spicer SS. Diamine methods for differentialing mucosubstances histochemically. J Histochem Cytochem 1965;13:211–234.

**Received May 31, 2021. Accepted August 19, 2021.**

**Correspondence**
Address correspondence to: James R. Goldenring, MD, PhD, AGAF, Epithelial Biology Center, Vanderbilt University Medical Center, MRB IV 10435G, 2213 Garland Avenue, Nashville, Tennessee 37232-2733. e-mail: jim.goldenring@vumc.org; fax: (615) 343-1591.

**CRediT Authorship Contributions**

Su-Hyung Lee, DVM, PhD (Conceptualization: Equal; Data curation: Lead; Formal analysis: Lead; Investigation: Lead; Methodology: Equal; Writing – original draft: Lead; Writing – review & editing: Equal)

Bogun Jang, MD, PhD (Data curation: Equal; Formal analysis: Lead; Investigation: Equal; Methodology: Equal; Writing – review & editing: Equal)

Jimin Min, PhD (Data curation: Equal; Formal analysis: Equal; Investigation: Equal; Methodology: Equal; Writing – review & editing: Equal)

Ela W. Contreras-Panta, BS (Data curation: Supporting; Formal analysis: Supporting; Investigation: Supporting; Methodology: Supporting; Writing – review & editing: Supporting)

Kimberly S. Presentation, BS (Investigation: Supporting; Methodology: Supporting; Writing – review & editing: Supporting)

Alberto G. Delgado (Investigation: Supporting; Methodology: Supporting; Writing – review & editing: Supporting)

M. Blanca Piazuelo, MD (Formal analysis: Supporting; Investigation: Supporting; Supervision: Supporting; Validation: Supporting; Writing – review & editing: Supporting)

Eunyoung Choi, PhD (Conceptualization: Supporting; Formal analysis: Supporting; Funding acquisition: Supporting; Investigation: Supporting; Methodology: Supporting; Supervision: Supporting; Writing – review & editing: Supporting)

James R. Goldenring, MD, PhD (Conceptualization: Lead; Formal analysis: Equal; Funding acquisition: Lead; Supervision: Lead; Writing – review & editing: Equal)

**Conflicts of interest**
The authors disclose no conflicts.

**Funding**
Supported by grants from Department of Veterans Affairs Merit Review Award IBX000930, DOD CA160479, NIH R01 DK071590, and R01 DK101332 and Cancer UK Grand Challenge Award 29075 (to J.R.G), DOD CA160399, NIH R37 CA244970, and pilot funding from VICC GI SPORE P50CA236733 (to E.C), National Research Foundation of Korea (NRF) grant funded by the Korea government (MSIT) (No. 2021R1C1C1011172) (to B.G.), and DOD CA191242 (to J.M). Supported by core resources of the Vanderbilt Digestive Disease Center (NIH P30 DK058404) and Vanderbilt Ingram Cancer Center (P30 CA068485) with imaging in the Vanderbilt Digital Histology Shared supported by a VA Shared Instrumentation grant (1IS1BX003097).